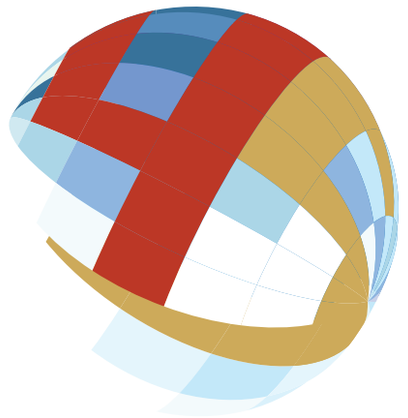

NUMERICAL WEATHER AND CLIMATE MODELING

Beginnings, Now, and Vision of the Future

НУМЕРИЧКО МОДЕЛИРАЊЕ ВРЕМЕНА И КЛИМЕ

Почеци, садашњост и визија будућности

10. септембар 2018. у 10 сати
Кнез Михаилова 35, Свечана сала САНУ

SERBIAN ACADEMY OF SCIENCES AND ARTS

NUMERICAL WEATHER AND CLIMATE MODELING

BEGINNINGS, NOW, AND VISION OF THE FUTURE

BELGRADE, SEPTEMBER 10, 2018

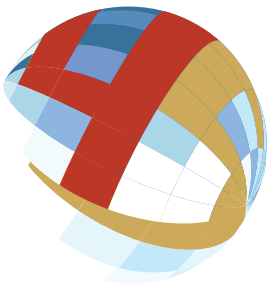

Organizing Committee:

Members:

Zoran Knežević
Serbian Academy of Science and Arts, Serbia

Aleksandra Kržič
Republic Hydrometeorological Service of Serbia

Fedor Mesinger
Serbian Academy of Science and Arts, Serbia

Jugoslav Nikolić
Republic Hydrometeorological Service of Serbia

Katarina Veljović
University of Belgrade – Faculty of Physics, Serbia

Ana Vuković
University of Belgrade – Faculty of Agriculture, Serbia

PROGRAM

Belgrade, September 10, 2018

10:00–10:20 **Opening addresses**

10:20–10:45 **The ECMWF model dynamical core and visions of its future**

Michail Diamantakis, P. Bauer, W. Deconinck, P. Dueben, C. Kuenhlein, S. Malardel, A. Mueller, P. Smolarkiewicz, F. Vana, and N. Wedi

10:45–11:10 **Dynamical cores for the Met Office's Unified Modelling system: Past, present and future**

Nigel Wood

11:10–11:35 **Numerical Modeling of the Atmosphere: A Review**

Miodrag Rančić, and Fedor Mesinger

11:35–12:00 Coffee break

12:00–12:20 **Overview of the KIAPS's next generation global model (KIM; Korea Integrated Model)**

Young C. Kwon, Song-You Hong, and KIAPS coauthors

12:20–12:40 **Global multi-scale atmosphere model SL-AV**

Mikhail Tolstykh, Rostislav Fadeev, Vladimir Shashkin, and Gordey Goyman

12:40–13:00 **Atmospheric dust modeling - A way to better understand the Earth system**

Bojan Cvetkovic, Goran Pejanovic, Slobodan Nickovic, Ana Vukovic, Mirjam Vujadinovic Mandic, Vladimir Djurdjevic, and Jugoslav Nikolic

13:00–14:30 Lunch break

14:30–14:50 **Cut-cell Eta: Some history, and lessons from its present skill**

Fedor Mesinger, and Katarina Veljovic

14:50–15:10 **From subseasonal to seasonal forecasts over South America using the Eta Model**

Sin-Chan Chou, Nicole Resende, Maria Luiza da Rocha, Claudine P. Dereczynski, Jorge Luís Gomes, and Gustavo Sueiro

15:10–15:30 **The CMCC Operational Seasonal Prediction Modelling System**

Stefano Tibaldi, Antonella Sanna, Andrea Borrelli, Davide Padeletti, Silvio Gualdi, and Antonio Navarra

15:30–16:10 **Poster session** including Coffee break

Posters:

1-km Eta Model Simulations over Complex Topography

Jorge Luis Gomes, Daniela Carneiro Rodrigues, and Sin-Chan Chou

Coupled modeling system in a seamless prediction approach

Bojan Cvetkovic, Goran Pejanovic, Vladimir Djurdjevic, Ana Vukovic, Mirjam Vujadinovic Mandic, Aleksandra Krzic, Slobodan Nickovic, Slavko Petkovic, and Jugoslav Nikolic

16:10–16:30 **Development and evaluation of Global Eta Framework (GEF) model at medium and seasonal ranges**

Dragan Latinovic, Sin-Chan Chou, Miodrag Rančić, Jonas Tamaoki, Gustavo Sueiro, Jorge Gomes, and André Lyra

16:30–16:50 **Cloud parameterization and cloud prediction scheme in the Eta numerical weather model**

Ivan Ristic, and Ivana Kordic

16:50–17:20 **Towards revision of conventional theory and modelling of turbulence in boundary-layer flows**

Sergej S. Zilitinkevich, and **Evgeny Kadantsev**

17:20–17:45 **Concluding words and Discussion**

ABSTRACTS

From subseasonal to seasonal forecasts over South America using the Eta Model

Sin-Chan Chou[1], Nicole Resende[1], Maria Luiza da Rocha[2], Claudine P. Dereczynski[2], Jorge Luís Gomes [1], and Gustavo Sueiro[1]

[1] CPTEC – Center for Weather Forecasts and Climate Studies, INPE – National Institute for Space Research, Cachoeira Paulista, SP, Brazil (chou.chan@inpe.br)

[2] IGEO – Geosciences Institute, UFRJ – Federal University of Rio de Janeiro, Rio de Janeiro, RJ, Brazil.

Introduction

Forecasts at seasonal and sub-seasonal time ranges are useful for planning actions in various socio-economic sectors such as energy, agriculture, water supply, etc. Higher spatial resolution forecasts are more suitable for dealing with local problems. However, the skill of the seasonal forecasts are generally limited and the skill of subseasonal forecasts of little knowledge. Therefore, to investigate the level of the forecast skill are crucial for making the information useful.

The objective of this work is to evaluate the Eta model skill for seasonal and sub-seasonal forecasts over South America.

The Eta model

The Eta model (Mesinger et al. 2012; Mesinger et al. 1988; Black 1994; Janjić 1994) has been used by the Center for Weather Forecasts and Climate Studies (CPTEC) to provide operational weather forecasts for South America since 1996 (Chou, 1996). One of the major feature of the model is the vertical eta coordinate, or the so-called step-mountain coordinate (Mesinger 1984). The reason for the choice of the Eta model at CPTEC was the advantage of the eta over the sigma coordinate to reproduce the summer circulation over South America (Figueroa, 1992). The major windstorm, the zonda wind, is reproduced accurately by the Eta model (Seluchi et al., 2003; Antico et al. 2017)) at different temporal scales. The model is setup at 40 km and 15 km resolution, for medium range forecasts, 5 km over Southeast Brazil for high-resolution ensemble forecasts, and 1-km for power plant emergency forecasts.

Seasonal forecasts started operationally in 2002 (Chou et al. 2005) and a modified version for climate change studies was developed (Pesquero et al. 2010; Chou et al. 2012; Chou et al. 2014) to support various impact, vulnerability, and adaptation studies (MCTI, 2016; Tavares et al. 2017). The upgraded version of the model (Mesinger et al. 2012) includes the 'cut-cell' feature for the coordinate, the piecewise linear scheme for vertical advection, among other features. The model versions use the Betts-Miller-Janjic (Janjić 1994) scheme for cumulus parameterization, Ferrier (Ferrier et al. 2002) or Zhao (Zhao et al. 1997) scheme for cloud microphysics parameterization, GFDL radiation package which

parameterizes long (Schwarzkopf and Fels 1991) and short waves (Lacis and Hansen 1974), and the NOAH land-surface scheme (Ek et al. 2003).

These features are incorporated in the updated version for seasonal forecasts (Chou et al. 2018) and for subseasonal forecasts.

The seasonal forecasts

The domain adopted for the seasonal forecasts encompasses the entire South America and Central America continents (Figure 1). Model resolution is 40 km in the horizontal and 38 layers in the vertical. The forecast length is 4 months, and an additional approximately 0.5-month for land-surface spin-up time. Five ensemble members are constructed by assuming small perturbations in the initial conditions, which consider model runs starting between the dates 13 and 17 of month before the forecast season. For example, the model forecast run for the season October-November-December-January (ONDJ) starts on September 13, 14, 15, 16, and 17. The Eta model is driven by the CPTEC global atmospheric model at T62L28 resolution, and uses the persisted sea surface temperature anomaly.

Over the most part of the continent, the seasonal precipitation forecasts are underestimated, especially during the rainy season. On the other hand, overestimate of seasonal precipitation is forecast over the equatorial Intertropical Convergence Zone (ITCZ) region, along the eastern coast of the continent and along the eastern slopes of the tropical Andes mountains.

A single member of the forecast run driven by the CPTEC Coupled Ocean-Atmosphere global model show some reduction of these systematic seasonal precipitation errors.

Considering the increase of spatial resolution provided by the Eta regional climate model (RCM), Figure 2 explores the use of the increased temporal resolution for the upper Sao Francisco river basin located in Southeast Brazil. Monthly precipitation for the season OND averaged over 7 years is compared against two observational dataset. The comparison shows that the monthly precipitation forecasts reproduce the increasing trend of precipitation, but underestimate the amounts in all months. In addition, the forecast run driven by the OAGCM show some reduction of the underestimate error. The improvement of these precipitation forecasts using the OAGCM have also been shown by Pilotto et al. (2012).

The subseasonal forecasts

The subseasonal forecasts produced by the Eta model for 50 days ahead are driven by the CPTEC OAGCM forecasts at T62L28 resolution, and the respective forecasted sea surface temperature. The 20 members of the ensemble are constructed as lagged-ensemble forecasts. This is done by taking the initial conditions 10 days before and running at 00 Z and 12 Z, for 60-day integration length. The Eta model was setup at 40-km resolution. Figure 3 shows the 10-day accumulated precipitation in the São Francisco river basin for the period between February 10 and March 31, 2015. Therefore, the initial conditions were taken for

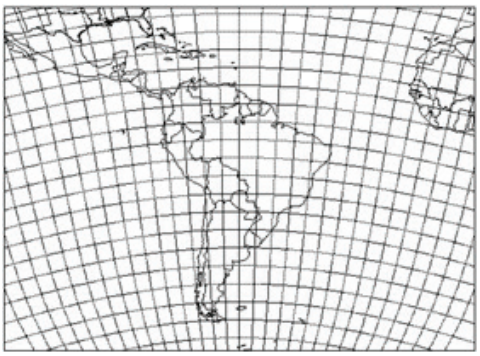

Figure 1 – Model domain for the Eta seasonal forecasts.

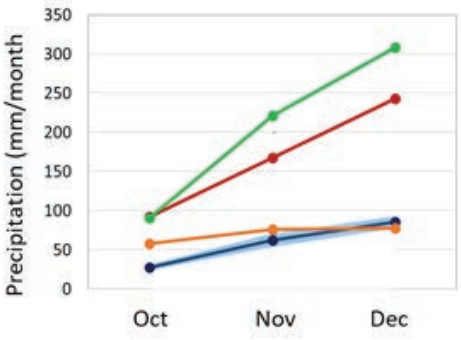

Figure 2 – Seasonal Precipitation (mm/month) forecasts for the months of October, November, and December, averaged over the years between 2001 and 2007. The curves are CRU (red), CMORPH (green), Eta-OAGCM (orange), and Eta-AGCM (blue).

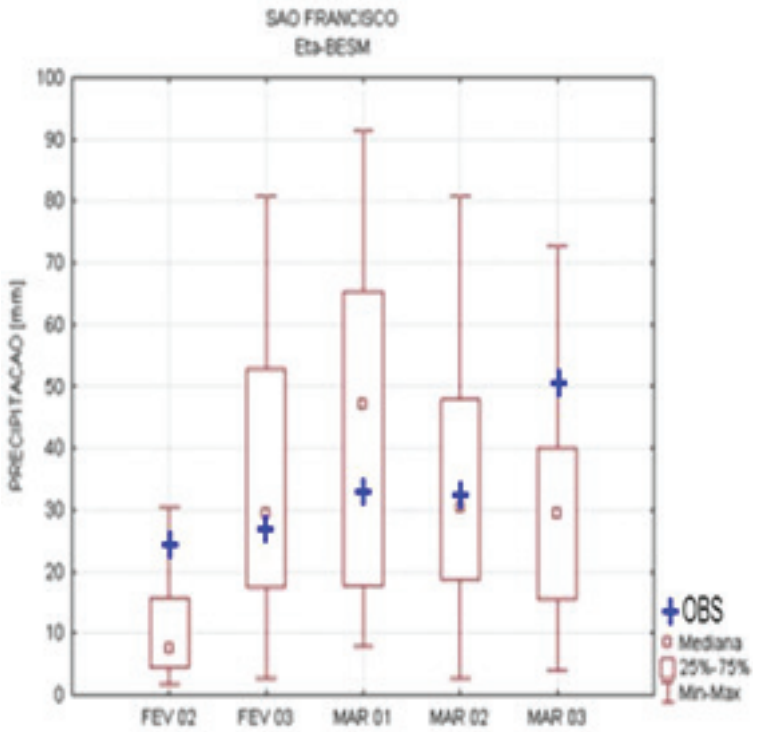

Figure 3 – Boxplot of subseasonal (50-day) precipitation (mm/10day) forecasts in the Sao Francisco basin, between Feb. 10 and Mar. 31, 2015. Observations are indicated in crosses.

the period between February 1st and 9th, 2015.

Unlike the seasonal forecasts, subseasonal forecast over Sao Francisco river basin does not show large underestimate. The forecasts between the second and the fourth 10-day period show reasonable agreement with observations as these values lie within the 25th and 75th percentile. The first and fifth period show precipitation underestimate. For the month of March, the total precipitation forecast is about 108 mm whereas observation is 101 mm and observed climatology for the month is 136 mm for the basin. Therefore, these forecasts show potential for useful in planning activities.

Conclusions

The Eta model runs at CPTEC/INPE for high-resolution weather forecasts, for ensemble forecasts, at short and medium ranges. Here some evaluations of Eta model precipitation forecasts at seasonal and sub-seasonal ranges are shown. The lateral boundary condition are crucial for seasonal range as precipitation errors patterns change. The seasonal forecasts have reduced errors when driven by the CPTEC OAGCM. At sub-seasonal range, the precipitation errors tend to show different pattern and no clear underestimate. Additional seasonal range runs produced by modifying Eta model physics are being evaluated and considered as candidates for ensemble members. At sub-seasonal ranges, higher spatial resolution may improve the forecast skill. The construction of hindcasts is ongoing. Despite the errors, the precipitation forecasts have shown potential for planning applications.

References

Antico PL, Chou SC, Mourão C (2017) Zonda downslope winds in the central Andes of South America in a 20-year climate simulation with the Eta model. Theor Appl Climatol 128:291–299. doi: 10.1007/s00704-015-1709-2

Black TL (1994) The new NMC mesoscale Eta model: Description and forecast examples. Weather Anal Forecast 9:265–278

Chou SC (1996) Modelo Regional Eta. Climanalise. Edição Comemorativa. INPE. São José dos Campos, SP, Brazil.

Chou SC, Bustamante JF, Gomes JL (2005) Evaluation of Eta Model seasonal precipitation forecasts over South America. Nonlinear Process Geophys 12:537–555. doi: 10.5194/npg-12-537-2005

Chou SC, Dereczynski CP, Gomes JL, et al (2018) Ten—year seasonal climate reforecasts over South America using the Eta Regional Climate Model. Ann Brazilian Acad Sci

Chou SC, Lyra A, Mourão C, et al (2014) Assessment of Climate Change over South America under RCP 4.5 and 8.5 Downscaling Scenarios. Am J Clim Chang 3:512–527. doi: 10.4236/ajcc.2014.35043

Chou SC, Marengo JA, Lyra AA, et al (2012) Downscaling of South America present climate driven by 4-member HadCM3 runs. Clim Dyn 38:635–653. doi: 10.1007/s00382-011-1002-8

Ek M, Mitchell FB, Liu Y, et al (2003) Implementation of Noah Land Model advances in the NCEP operational Eta Model. J Geophys Res 108:8851–8867

Ferrier BS, Lin Y, Black T, et al (2002) Implementation of a new grid-scale cloud and precipitation scheme in the NCEP Eta model. In: 15th Conference on numerical weather prediction, American Meteorological Society. San Antonio, TX, pp 280–283

Janjić ZI (1994) The step-mountain coordinate model: further developments of the convection, viscous sublayer, and turbulence closure schemes. Mon Weather Rev 112:927–945

Lacis AA, Hansen JE (1974) A parameterization of the absorption of solar radiation in the earth's atmosphere. J Atmos Sci 31:118–133

Mesinger F (1984) A blocking technique for representation of mountains in atmospheric models. Riv Meteorol Aeronaut 44:195–202

Mesinger F, Chou SC, Gomes JL, et al (2012) An upgraded version of the Eta model. Meteorol Atmos Phys 116:63–79. doi: 10.1007/s00703-012-0182-z

Mesinger F, Janjić ZI, Nickovic S, et al (1988) The step-mountain coordinate: Model description, and performance for cases of Alpine lee cyclogenesis and for a case of an Appalachian redevelopment. Mon Weather Rev 116:1493–1518

Pesquero JF, Chou SC, Nobre CA, Marengo JA (2010) Climate downscaling over South America for 1961-1970 using the Eta Model. Theor Appl Climatol 99:75–93. doi: 10.1007/s00704-009-0123-z

Pilotto IL, Chou SC, Nobre P (2012) Seasonal climate hindcasts with Eta model nested in CPTEC coupled ocean-atmosphere general circulation model. Theor Appl Climatol 110:437–456. doi: 10.1007/s00704-012-0633-y

Schwarzkopf MD, Fels SB (1991) The simplified exchange method revisited: an accurate, rapid method for computation of infrared cooling rates and fluxes. J Geophys Res 96:9075–9096

Seluchi ME, Norte FA, Satyamurty P, Chou SC (2003) Analysis of three situations of Foehn effect over the Andes (Zonda wind) using the Eta/CPTEC regional model. Weather Anal Forecast 18:481–501

Tavares S, Giarolla A, Chou SC, et al (2017) Climate change impact on the potential yield of Arabica coffee in southeast Brazil. Reg Environ Chang 1:1–11

Zhao Q, Black TL, Badwin ME (1997) Implementation of the cloud prediction scheme in the Eta Model at NCEP. Weather Forecast 12:697–712

Coupled modeling system in seamless prediction approach

Bojan Cvetkovic[1], Goran Pejanovic[1], Vladimir Djurdjevic[2], Ana Vukovic[3], Mirjam Vujadinovic Mandic[3], Aleksandra Krzic[1], Slobodan Nickovic[1], Slavko Petkovic[1] and Jugoslav Nikolic[1]

[1] Republic Hydrometeorological Service of Serbia - South East European Climate Change Center (RHMSS/SEEVCCC), Belgrade, Serbia (bojan.cvetkovic@hidmet.gov.rs)
[2] Institute of Meteorology, Faculty of Physics, University of Belgrade, Belgrade, Serbia
[3] Faculty of Agriculture, University of Belgrade, Belgrade, Serbia

The coupled Seasonal Ensemble Prediction System (EPS)

Since the early 20th century, when the concept of numerical weather prediction (NWP) was firstly introduced, it has gone through dramatic changes and improvement. The essence idea of resolving a large number of governing thermodynamic equations, describing the atmospheric processes of wide spatial and time scales, requires enormous computational resources. Evolution of the new theories and development of supercomputers rapidly lead to tremendous progress of models. The seasonal ensemble prediction system (EPS), as probably the most demanding of all, requires thousands of processors since a large number of various models (ocean, land-surface, radiation, microphysics, dynamics etc.) are working synchronously within the same frame. Taking into consideration the length of the integration (several months for seasonal and several decades for the climate integrations), along with high demands regarding better resolution and ensemble approach, clearly illustrates the complexity of these systems. Following the well routed tradition in research and modelling, RHMS and Belgrade University continues to cooperatively develop several models, both for short and long range forecasts.

The aim of this paper is to summarize, review and discuss the current status of seasonal and climate prediction modeling system at the RHMSS/SEEVCCC (Republic Hydrometeorological Service of Serbia/South East European Climate Change Center), and also to provide the information on ongoing operational and research progress.

The first model to be in operational use was regional Eta model (Mesinger et al., 1988), primarily implemented for the short-range forecast. Further improvements lead to coupling it with the Princeton Ocean Model (POM) (Blumberg, A.F. and G.L. Mellor, 1987) in order to perform the seasonal forecast. The current operational ensemble seasonal prognostic system is based on the dynamical downscaling of ECMWF System 4 and System 5 seasonal forecast, using regional two-way coupled atmosphere-ocean EBU-POM model (Djurdjevic and Rajkovic, 2008; Djurdjevic and Rajkovic, 2010). Following the ensemble approach in order to quantify the

forecast uncertainties, the 51 ensemble member has been introduced into operational use in June 2009.

Modeling climate change and impacts

The future strategic planning in economic development and therefore impact analysis, which requires high level of confidence, significantly relies on climate model simulations and impact studies. This paper also reports on research related to climate change and impacts in Serbia, resulted from cooperative work of the modeling and user community. Dynamical downscaling of climate projections for the 21st century with multi-model approach and statistical bias correction applied, provided model results for impact studies. Presented results are from simulations performed using regional EBU-POM model, forced with A1B and A2 SRES/IPCC (2007), along with comparative analysis with other regional models and results from the latest high-resolution NMMB (Nonhydrostatic Multiscale Model on the B Grid) (Janjic, 2010; Janjic, 2012.) simulations forced with RCP8.5 IPCC scenario (2012).

Earth Modeling System (EMS)

According to the IPCC reports, the largest uncertainty in defining radiative forcing in climate modelling and projections is linked with the aerosols, especially with mineral dust. The latest research and improvements in regional atmospheric-dust coupled model NMME-DREAM (Dust Regional Atmospheric Model) (Nickovic, 2001; Nickovic, 2004; Pejanovic et al., 2012; Vukovic et al., 2014), has shown mineral dust particles to have possibly the most important role in process of the cold clouds heterogeneous ice nucleation, consequently influencing the radiative effects and precipitation forecast (Nickovic et al., 2016).

Already implemented in the regional NMME DREAM (fully operational at RHMS/SEEVCCC and WMO SDS-WAS since 2012) and global NMMB model, this finding imposed an idea of constructing a new Subseasonal-to-Seasonal (S2S) system, which we are developing within ongoing special project at the European Centre for Medium-Range Weather Forecasts (ECMWF), named 'Mineral Aerosol Impacts to Sub-seasonal to Seasonal Predictability - MASP'. This system consists of Dust Regional Atmospheric Model – DREAM, driven by the NMM atmospheric model (Janjic et al., 2001) and coupled with the POM ocean model (Djurdjevic and Rajkovic, 2008).

References

Blumberg, A.F., and G.L. Mellor, A description of a three-dimensional coastal ocean circulation model, in Three-Dimensional Coastal Ocean Models, Vol. 4, edited by N.Heaps, pp. 208, American Geophysical Union, Washington, D.C., 1987.

Djurdjevic, V. and Rajkovic, B. (2010), Development of the EBU-POM coupled regional climate model and results from climate change experiments, In: Advances in Environmental Modeling and Measurements, Editors: T. D. Mihajlovic and Lalic B., Nova Publishers.

Djurdjevic V. and Rajkovic, B. (2008), Verification of a coupled atmosphere-ocean model using satellite observations over the Adriatic Sea, Annales Geophysicae, 26(7): 1935-1954.

Janjic, Z. I., and R. Gall, 2012: Scientific documentation of the NCEP Nonhydrostatic Multiscale Model on the B Grid (NMMB). Part 1: Dynamics. NCAR/TN-489+STR, 75 pp. http://nldr.library.ucar.edu/repository/assets/technotes/TECHNOTE-000-000-000-857.pdf.

Janjic, Z. I., 2010: Recent advances in global nonhydrostatic modeling at NCEP. Proc. Workshop on Non-hydrostatic Modelling, ECMWF, Reading, United Kingdom. http://nwmstest.ecmwf.int/newsevents/meetings/workshops/2010/Non_hydrostatic_Modelling/presentations/Janjic.pdf.

Janjic, Z. I.: A Nonhydrostatic Model Based on a New Approach, Meteorol. Atmos. Phys., 82, 271–285, doi:10.1007/s00703-001-0587-6, 2003.

Mesinger, F., Z.I. Janjic, S. Nickovic, D. Gavrilov and D.G. Deaven, 1988: The steep-mountain coordinate: Model description and performance for cases of Alpine lee cyclogenesis and for a case of an Appalachian redevelopment. Mon. Wea. Rew., 116, 1493-1518

Nickovic, S., Cvetkovic, B., Madonna, F., Rosoldi, M., Pejanovic, G., Petkovic, S., and Nikolic, J.: Cloud ice caused by atmospheric mineral dust – Part 1: Parameterization of ice nuclei concentration in the NMME-DREAM model, Atmos. Chem. Phys., 16, 11367-11378, doi:10.5194/acp-16-11367-2016, 2016. http://www.atmos-chem-phys.net/16/11367/2016/acp-16-11367-2016.pdf

Nickovic S. (2004), Interactive Radiation-Dust Model: A Step to Further Improve Weather Forecasts (invited presentation). International Symposium on Sand and Dust Storm, Beijing, China, 12-14 September 2004.

Nickovic, S., Kallos, G., Papadopoulos, A., and Kakaliagou, 2001, O.: A model for prediction of desert dust cycle in the atmosphere, J. Geophys. Res., 106, 18113–18130, 2001.

Pejanovic, G., S. Nickovic, M. Vujadinovic, A. Vukovic, V. Djurdjevic, M. Dacic, Atmospheric deposition of minerals in dust over the open ocean and possible consequences on climate. WCRP OSC Climate Research in Service to Society, 24-28 October 2011, Denver, CO, USA

Vukovic, A., Vujadinovic, M., Pejanovic, G., Andric, J., Kumjian, M. R., Djurdjevic, V., Dacic, M., Prasad, A. K., El-Askary, H. M., Paris, B. C., Petkovic, S., Nickovic, S., and Sprigg, W. A.: Numerical simulation of "an American haboob", Atmos. Chem. Phys., 14, 3211-3230, https://doi.org/10.5194/acp-14-3211-2014, 2014.

Atmospheric dust modeling - A way to better understand the Earth system

Bojan Cvetkovic[1], Goran Pejanovic[1], Slobodan Nickovic[1], Ana Vukovic[2], Mirjam Vujadinovic Mandic[2], Vladimir Djurdjevic[3] and Jugoslav Nikolic[1]

[1] Republic Hydrometeorological Service of Serbia - South East European Climate Change Center (RHMSS/SEEVCCC), Belgrade, Serbia (bojan.cvetkovic@hidmet.gov.rs)
[2] Faculty of Agriculture, University of Belgrade, Belgrade, Serbia
[3] Institute of Meteorology, Faculty of Physics, University of Belgrade, Belgrade, Serbia

Dust process and impacts

Several megatons of mineral dust are annually emitted into the atmosphere through sporadic dust storms by strong near-surface winds over the various arid regions. Dust particles of microns size can be transported downwind thousands of kilometers away from sources.

Mineral dust is an essential climate and environmental variable. It plays a key role in the Earth system. It affects the atmospheric energy balance and acts on timescales of minutes to millennia and space scales from micro to global. Dust influences radiation and clouds and consequently also precipitation. Iron and other mineral nutrients carried by dust fertilize both terrestrial and marine environments. In regions close to dust sources, it adversely affects human health and ground transport and aviation.

Therefore, there were numerous reasons why in late the 80-ties of the last century the interest to better understand the atmospheric dust process, but also to monitor and to predict/simulate it, has rapidly gown. That time dust modeling was in infant phase; today tents of dust models are today available in the research and prediction community. Interestingly, Lewis Fry Richardson (1922), in his attempt to developed the first numerical weather prediction (NWP) system added the atmospheric dust as an eighth variable (Edwards 2000).

Following the interest of more than 40 member countries, WMO (World Meteorological Organization) launched the Sand and Dust Storm Warning Advisory and Assessment System (SDS-WAS), whose mission is to enhance the ability of countries to deliver timely and quality dust forecasts, observations, information and knowledge to users through an international partnership of research and operational communities.

Dust Regional Atmospheric Model (DREAM)

In the beginning of 1990-ties, the first ever successful dust forecast has been performed by the DREAM precursor (Nickovic, 1996), in which the dust component has been online driven by the NCEP/Eta atmospheric model. DREAM has been continuously improving by introducing components such as: new NCEP/NMM nonhydrostatic atmospheric model driver; distribution of eight particle sizes; detailed description of

dust sources; mineralogical composition of dust; indirect (dust-clouds) and direct (dust-radiation) feedback mechanisms. DREAM is designed to simulate all major processes of the atmospheric dust cycle: dust emission, turbulent diffusion, vertical and horizontal advection, lateral diffusion, and wet and dry deposition (Nickovic et al., 2001; Nickovic, 2002, 2003, 2004; Pejanovic et al., 2010). Dust concentration is one of the NMM governing prognostic equations which solve a set of dust mass continuity equations for eight particle size classes which radii range from 0.15 to 7.1 μm.

The main difference between DREAM and other dust models is that the DREAM dust emission parameterization applies a viscous sub-layer concept (Janjic, 1994) for treating mass–heat–momentum exchanges between the surface and the lowest model layer. In DREAM, this component regulates the intensity of dust turbulent transfer into the lowest model layer accounting for different turbulent regimes (laminar, transient and turbulent mixing), and using the surface dust concentration as the lower boundary condition. Parameterization of the wet removal is done with a parameterization method for wet deposition involving rainfall rate and washout ratio (Nickovic et al, 2001). Dry deposition on the surface is based on a scheme which includes deposition due to turbulent and Brownian diffusion, gravitational settlement, and interception and impaction of particles by surface roughness elements.

Dust emission is among the most critical components in dust modeling. From its accuracy the successful description of other dust processes very much depends. If there are favorable near-surface conditions, the modeled dust emission is usually calculated from predefined sources. Most of current models (including the standard DREAM version) applied for continental deserts use the prescribed dust source function proposed by Ginoux et al., (2001) which depends on topography structures and vegetation cover. It represents the fraction of alluvium available for wind erosion.

DREAM is one of the twelve dust models participating in the WMO SDS-WAS model inter-comparison project. Nowadays, it represents the most used dust model in the international community, used for operational and forecasting purposes in more than 20 organizations.

Examples of DREAM implementation

This presentation reports on some recently developed DREAM model components and applications.

Dust particles as ice nuclei - Insoluble particles such as dust are known as one of the best ice nuclei. (Cziczo et al. 2013). Large interest on ice nucleation research is today motivated, inter alias, by needs of the community to improve unsatisfactory representation of cloud formation in atmospheric models, and therefore to increase the accuracy of weather and climate predictions. Most of today's models use either climatological dust concentration or pre-specified number of dust ice nuclei. We used a new generation of ice nucleation parameterizations (DeMott et al., 2015; Steinke et al., 2015) to developed a a method to calculate ice nucleation due to dust predicted DREAM which is input into the cloud

microphysics of the atmospheric model driver (Nickovic et al., 2016).

Dust mineralogy - Mineral composition of dust affects various processes such as the atmospheric, ocean and terrestrial environments, as well as human health. Including mineral dust transport interacting with the atmosphere in numerical models can improve accuracy of weather forecasts and climate simulations and can contribute to better understanding of the environmental processes caused by mineral dust. We have therefore developed a database of geographical distribution of 8 typical minerals present in dust-productive soils mapped in a 30-sec grid (GMINER30) (Nickovic at al., 2012). This database could be used as input data for various dust model applications. GMINER30 has been used to parameterize the atmospheric chemical processing of iron minerals carried by dust (Nickovic et al, 2013) which, when deposited into the ocean environment, represent the major marine micronutrient.

Dust prediction from high latitude dust sources - Recent study of Cvetkovic et al., (2018) describes a DREAM version applied over the Icelandic dust sources. Iceland as the largest European source of mineral dust in the Arctic region. The geochemistry of its dust is characterized by high iron content, usually about 10% Fe, which is much higher than in continental dust in general. The iron as an essential micronutrient for marine microbial organisms is important modulator of the high latitude North Atlantic ability to uptake atmospheric CO2, thus contributing to deceleration of the ongoing Arctic seawater acidification. In recent years, the high latitude North Atlantic Ocean has become a focus for research into the role of Fe in ocean productivity (Achterberg et al., 2018). Our study aims to set a basis for future research on high latitude climate and environment responses to dust transport.

References

Achterberg, E.P., S. Steigenberger, C.M. Marsay, F.A.C. LeMoigne, S.C. Painter, A.R. Baker, D.P. Connelly, C.M.Moore, A. Tagliabue, and T. Tanhua, 2018: Iron Biogeochemistry in the High Latitude North Atlantic Ocean. Nature, Scientific Reports (2018) 8:1283, DOI:10.1038/s41598-018 19472-1.

Cvetkovic, B., S. Nickovic, S. Petkovic, P. Dagsson-Waldhauserova, O. Arnalds, A. Vukovic, G. Pejanovic, J. Nikolic. Prediction system for atmospheric process of Icelandic mineral dust (in preparation)

Cziczo, D.J., K.D. Froyd, C. Hoose, E.J. Jensen, M. Diao, M.A. Zondlo, J.B. Smith, C.H. Twohy, D.M. Murphy: Clarifying the Dominant Sources and Mechanisms of Cirrus Cloud Formation. Science, Vol. 340, Issue 6138, pp. 1320-1324,2013

DeMott, P. J., Prenni, A. J., McMeeking, G. R., Sullivan, R. C., Petters, M. D., Tobo, Y., Niemand, M., Möhler, O., Snider, J. R., Wang, Z., and Kreidenweis, S. M.: Integrating laboratory and field data to quantify the immersion freezing ice nucleation activity of mineral dust particles, Atmos. Chem. Phys., 15, 393-409, doi:10.5194/acp-15-393-2015, 2015.

Ginoux, P., Chin, M., Tegen, I., Prospero,

J., Holben, B.,Dubovik,O., and Lin, S. J.: Sources and distributions of dustaerosols simulated with the GOCART model, J. Geophys. Res.,106, 20255–20273, 2001.

Janjic, Z. I. (1994), The Step-mountain Eta Coordinate Model: Further developments of the convection, viscous sublayer and turbulence closure schemes, Mon. Weather Rev., 122, 927– 945.

Nickovic, S., Cvetkovic, B., Madonna, F., Rosoldi, M., Pejanovic, G., Petkovic, S., and Nikolic, J.: Cloud ice caused by atmospheric mineral dust – Part 1: Parameterization of ice nuclei concentration in the NMME-DREAM model, Atmos. Chem. Phys., 16, 11367-11378, https://doi.org/10.5194/acp-16-11367-2016, 2016.

Nickovic, S., Vukovic, A., and Vujadinovic, M.: Atmospheric processing of iron carried by mineral dust, Atmos. Chem. Phys., 13, 9169-9181, doi:10.5194/acp-13-9169-2013, 2013

Nickovic, S., A. Vukovic, M. Vujadinovic, V. Djurdjevic, and G. Pejanovic, Technical Note: High-resolution mineralogical database of dust-productive soils for atmospheric dust modeling Atmos. Chem. Phys., 12, 845–855, 2012 www.atmos-chem-phys.net/12/845/2012/ doi:10.5194/acp-12-845-2012

Nickovic, S., (2005), Distribution of dust mass over particle sizes: impacts on atmospheric optics, Forth ADEC Workshop - Aeolian Dust Experiment on Climate Impact, 26-28 January, Nagasaki, Japan, 357-360.

Nickovic, S., 2004: Interactive Radiation-Dust Model: A Step to Further Improve Weather Forecasts (invited presentation). International Symposium on Sand and Dust Storm, Beijing, China, 12-14 September2004.

Nickovic, S., 2002: Dust Aerosol Modeling: Step Toward Integrated Environmental Forecasting (Invited paper), Eos. Trans. AGU, 83(47), Fall Meet. Suppl., Abstract A71E-04, 2002.

Nickovic, S., G. Kallos, A. Papadopoulos, O. Kakaliagou, 2001: A model for prediction of desert dust cycle in the atmosphere J. Geophys. Res. 106, 18113-18130

Nickovic, S., 1996: Modelling of dust process for the Saharan and Mediterranean area. In: The impact of African dust across the Mediterranean, Eds: S. Guerzoni, and R. Chester, 1996 Kluwer Academic Publishers, Dordrecht., 15-23.

Pejanovic, G., S. Nickovic, M. Vujadinovic, A. Vukovic, V. Djurdjevic, M. Dacic, Atmospheric deposition of minerals in dust over the open ocean and possible consequences on climate. WCRP OSC Climate Research in Service to Society, 24-28 October 2011, Denver, CO, USA

Steinke, I., Hoose, C., Möhler, O., Connolly, P., and Leisner, T.: A new temperature- and humidity-dependent surface site density approach for deposition ice nucleation, Atmos. Chem. Phys., 15, 3703-3717, doi:10.5194/acp-15-3703-2015, 2015.

The ECMWF model dynamical core and visions of its future

M. Diamantakis[1], P. Bauer[1], W. Deconinck[1], P. Dueben[1], C. Kuenhlein[1], S. Malardel[2], A. Mueller[1], P. Smolarkiewicz[1], F. Vana[1], N. Wedi[1]

[1] ECMWF, Shinfield Park, Reading, RG2 9AX (michail.diamantakis@ecmwf.int)
[2] Meteo-France, Direction Interrégionale de Météo-France pour l'Océan Indien, 50 Boulevard du Chaudron – 97490 Sainte-Clotilde, Reunion (sylvie.malardel@meteo.fr)

The necessity for weather predictions at exascale

The European Centre for Medium Range Weather Forecasts (ECMWF) produces a multitude of weather and environmental predictions: global deterministic and probabilistic weather forecasts for up to 15 days ahead, wave forecasts, atmospheric composition forecasts, flood forecasts, reconstructions of past climates (re-analysis project) and weather forecasts at the monthly and seasonal time scale. This is a highly demanding computational task given that many of these forecasts are executed twice per day.

The constant requirement to improve forecast accuracy drives numerical weather prediction (NWP) models towards more complex, realistic representations of physical processes and higher spatial and temporal resolutions. The latter is important for reducing truncation errors arising from the numerical solution of the underlying nonlinear system of PDEs that describe the atmospheric dynamics and for resolving more accurately flow near complex topographic features. These more powerful and computationally expensive models add further pressure on super-computing resources given that operational weather forecast runs are subject to a tight time constraint of approximately one hour. Developments in modern computer processor design dictate that running a model faster can only be achieved through increased parallelism. Therefore, ECMWF as well as other global weather prediction centres, are gradually pushed towards use of exascale super-computing platforms for operations and research. Efficiency, weak and strong scaling properties of algorithms, portability of computer code to accelerator technologies such as GPUs, have become more important than ever. They are stimulating new research and in some cases the design and development of entirely new dynamical cores based on numerical techniques that will run efficiently on future exascale machines.

The ECMWF model dynamical core

A dynamical core is a fundamental component for every NWP and climate model linking various atmospheric processes with the equations of motion of fluid dynamics. The ECMWF model IFS is based on a hydrostatic dynamical core

that uses a spectral transform, semi-implicit, semi-Lagrangian (SISL) method for solving the prognostic equations. A non-hydrostatic version exists, however, this is not currently used operationally at ECMWF.

The combination of the SISL time-stepping with the spectral transform approach offers a unique combination of efficiency and accuracy. The unconditional stability of the SISL method allows stable long timestep integrations with maximum CFL numbers much larger than 1. The high accuracy of the spectral spatial discretization and the good dispersion properties of the semi-Lagrangian advection scheme ensure that this happens without loss of accuracy. The use of a reduced grid enhances further efficiency and avoids the severe accumulation of grid-points near the poles which is a typical disadvantage of regular latitude-longitude grids. These advantages provide a great incentive to continue maintaining the spectral SISL approach in operations. However, there are known disadvantages and limitations of this approach and therefore the investigation of alternative numerical techniques is paramount.

Past research experiments have shown that the Legendre transforms and their inverse, used to transform prognostic equation fields from grid-point to spectral space and vice versa, become very expensive as convection permitting resolutions are approached. The introduction of a fast Legendre transform (Wedi et al, 2013) and the new reduced cubic octahedral grid (Malardel et al, 2016) have resulted in significant efficiency gains extending the life of the spectral transform approach. However, such optimizations will not be adequate to satisfy existing operational constraints for resolutions at 5km and beyond where cost rises further due to large global communication overheads both in spectral transform and the semi-Lagrangian advection method. Furthermore, the current constant coefficient approach for the spectral semi-implicit scheme, that allows a very cheap solution of the derived Helmholtz elliptic equation at each timestep, has an ultimate limit. At horizontal resolutions near 1km where orographic slopes exceed 50 degrees, the spectral non-hydrostatic code may become unstable while the lack of formal mass conservation in transport is an additional concern.

Future developments

To deal with these computational and scientific challenges in a non-disruptive way, minimizing development risk, a hybrid and flexible strategy has been adopted in ECMWF (Wedi et al, 2015). A key element of this strategy is to continuously support and improve the spectral transform semi-Lagrangian model while an alternative scalable, non-hydrostatic compact stencil dynamical core for the IFS is being developed. This is a 3D, non-hydrostatic, conserving finite-volume module (FVM, Smolarkiewicz et al., 2016, Smolarkiewicz et al., 2017) with semi-implicit time-stepping that uses the same grid as the current operational spectral IFS allowing direct comparisons with it. It includes moist thermodynamics and an interface with IFS parametrizations to allow use of the same physics package for both the current and the new dynamical core. Results from testing the FVM have been very

encouraging, showing that both dynamical cores achieve very similar results in standard idealized dry and moist cases despite employing different numerical methods and having a different mathematical formulation.

This effort is supported and complemented by various infrastructure and algorithmic improvements that can be applied to both the spectral and FVM dynamical core of the IFS. These are outlined below.

The development of the Atlas library (Deconinck et al, 2017), an object-oriented library for flexible NWP software developments is a major contribution towards a flexible, efficient and scalable IFS. So far, it has enabled complex developments such as the development of the new dynamical core FVM and of a multi-grid tracer advection package which combines elements from the two different dynamical cores. Furthermore, it is envisaged that it will allow to run seamlessly the IFS on accelerator technologies such as GPUs and will facilitate the implementation and testing of other compact stencil numerical techniques such as those based on discontinuous Galerkin methods.

Another important recent development is the release of a single-precision version of the entire IFS forecast model (Váňa et al, 2017). Remarkably, by reducing communication and computation cost it achieves time savings by approximately 40%, compared with double precision version, without any significant impact on forecast skill.

Additional testing and optimizations of the IFS numerical algorithms are investigated on diversely different hardware architectures (standard CPUs, GPUs, ARMs). To facilitate this activity, model components from the dynamical core (but also from the most expensive parametrizations) have been extracted to become simpler autonomous testing units like mini-apps which we call "dwarfs" inspired by the so call Berkeley dwarfs. This approach allows easy testing of existing model components and has become a platform for exchanging algorithmic improvements with our partners working in the EU funded project ESCAPE.

The ECMWF strategy of simultaneously investing in both the current spectral and the new FVM dynamical core is a complex and huge collaborative task. The flexibility of our approach serves well our aim to deliver a scalable and energy efficient earth system model for exascale super-computers given the rapid developments in computer hardware which constantly challenge our views on the scalability performance of the techniques used in the IFS. It helps ECMWF to be prepared for entirely different outcomes and to adapt its models so that they can run efficiently on the chosen future super-computing platform no matter what its architecture will be.

References

W. Deconinck, P. Bauer, M. Diamantakis, M. Hamrud, C. Kühnlein, P. Maciel, G. Mengaldo, T. Quintino, B. Raoult, P.K. Smolarkiewicz, N.P. Wedi, 2017: Atlas: A library for numerical weather prediction and climate modelling, Computer Physics Communications, Vol. 141, 188-204

S. Malardel, N. Wedi, W. Deconinck, M. Diamantakis, C. Kühnlein, G. Mozdzynski, M. Hamrud, and P. Smolarkiewicz, 2016: A new grid for the IFS, ECMWF Newsletter, Vol., 146., 23-28

P.K. Smolarkiewicz, C. Kühnlein, W.W. Grabowski, 2017: A finite-volume module for cloud-resolving simulations global atmospheric flows, J. Comput. Phys. 341, 208-229.

P.K. Smolarkiewicz, W. Deconinck, M. Hamrud, C. Kühnlein, G. Mozdzynski, J. Szmelter, N.P. Wedi, 2016: A finite-volume module for simulating global all-scale atmospheric flows, J. Comput. Phys. 315, 287-304

F. Váňa, P. Düben, S. Lang, T. Palmer, M. Leutbecher, D. Salmond and G. Carver, 2017: Single Precision in Weather Forecasting Models: An Evaluation with the IFS. Mon. Wea. Rev. doi: 10.1175/MWR-D-16-0228.1

NP Wedi, M. Hamrud, G. Mozdzynski, 2013: A fast spherical harmonics transform for global NWP and climate models, Monthly Weather Review, Vol. 141, 3450-3461

Wedi N.P., P. Bauer, W. Deconinck, M. Diamantakis, M. Hamrud, C. Kuehnlein, S. Malardel, K. Mogensen, G. Mozdzynski, P.K. Smolarkiewicz, 2015: The modelling infrastructure of the Integrated Forecasting System: Recent advances and future challenges, ECMWF TechMemo 760, Reading UK.

1-km Eta Model Simulations over Complex Topography

Jorge Luis Gomes[1], *Daniela Carneiro Rodrigues*[1], *and Sin Chan Chou*[1]

[1] National Institute for Space Research, Cachoeira Paulista, Brazil (jorge.gomes@inpe.br)

Introduction

The Eta model is used operationally by INPE at the Centre for Weather Forecasts and Climate Studies (CPTEC) to produce weather forecasts over South America since 1997. The model has gone through upgrades along these years. Recently CPTEC started to run the model for very high resolution forecasts, configured over a region of complex topography located near the coast of Southeast Brazil. The Eta model was configured with 1-km horizontal resolution and 50 layers. This Eta-1 km version is driven by the Eta-5 km, which in turn is driven by CFSR reanalysis. In order to prepare the model to run at these very high resolutions, adjustments were made in model horizontal diffusion and in cloud microphysics scheme parameters. The objective of this work is to adjust the precipitation production of the Eta model in horizontal resolution of 1-km through sensitivity tests.

Eta model characteristics and experiment setup

Eta model main characteristics

- Grid-point model (E-grid)
- Eta vertical coordinate (Mesinger, 1984),
- Prognostic variables: T, q, u, v, ps, TKE, cloud hydrometeors
- Convection: Betts-Miller scheme (Betts and Miller, 1986)
- Cloud microphysics: Ferrier scheme (Ferrier, 2002)
- Turbulence: Mellor Yamada 2.5; MO surface layer, Paulson functions
- Radiation: GFDL package, tendencies updated every hour,
- Land surface scheme: Noah scheme, 4 soil layers,
- Soil moisture: monthly climatology
- Albedo: seasonal climatology
- SST: observed

1-km Eta model experiment setup

The selected area to adjust the precipitation production of the model is located in the Southeast of Brazil (SEB) and comprises part of the States of São Paulo, Minas Gerais and Rio de Janeiro (Fig. 1).

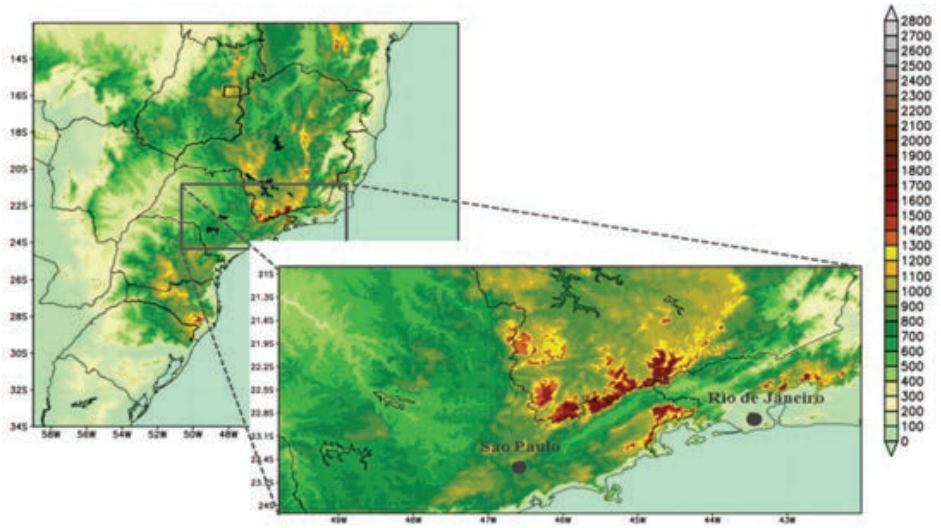

Fig. 1. 1-km Eta Model topography (m).

Selected case and experiments

In order to study only the effect of local surface conditions on the development of convective clouds and precipitation, case was chosen in which precipitation was initiated by convective instability due to surface and non-forced conditions.

The case occurred between 13 and 14 of February of 2013 over the selected area. Precipitation occurred associated with a summer storm without the influence of a large-scale forcing. Heavy rain happened in the late afternoon over the São Paulo city. The event starts around 17Z and dissipated around 22Z. The CMORPH 24-hour accumulated precipitation indicates intense precipitation near the São Paulo city (Fig. 2a).

Tests were performed with the precipitation production of the Eta model, Table 1 summarizes the experiments.

Table 1. Summary of sensitivity tests

Experiment	Description
Control	Cloud Microphysics Scheme is responsible for producing total precipitation.
BMJn90	The Betts Miller Janjic cumulus convection scheme was activated at the resolution of 1 km only for the convective mixture
Vsnow09	Terminal velocity of the ice crystal in the microphysics scheme was reduced by 25%.
Vsnow15	Terminal velocity of the ice crystal of the microphysics scheme was increased by 25%
RHgrd11	The relative humidity value to start cloud formation was change toward more restrictive value

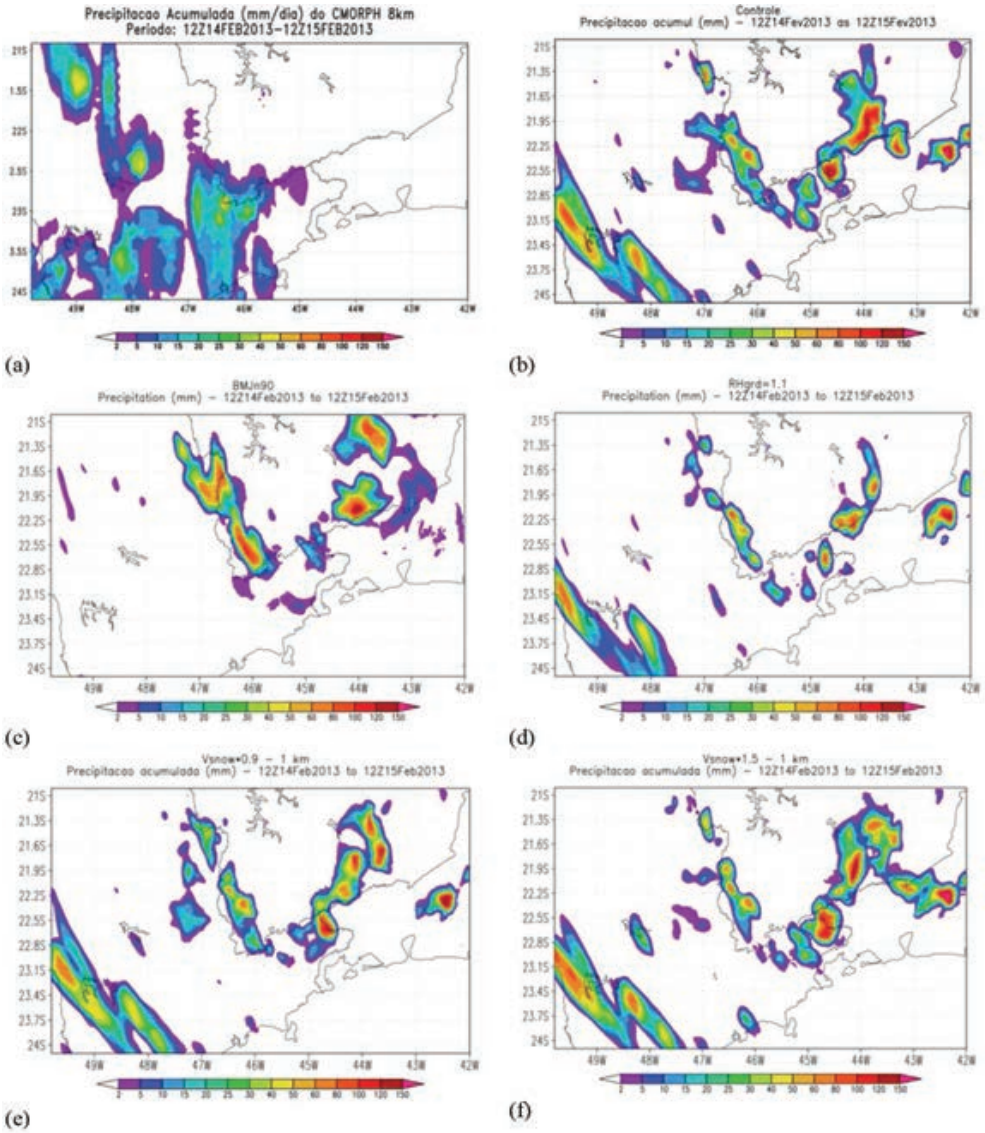

Fig. 2. 24-hour accumulated precipitation (mm), valid for February 14, 12Z. (a) CMORPH, (b) Control run, (c) BMJn90, (d) RHgrd1.1, (e) Vsnow0.9 and (f) Vsnow1.5.

Results

Fig. 2 (a-f) shows 24-hours accumulated precipitation for CMORPH and Control, RHgrd11, Vsnow09 and Vsnow15 experiments. When compared with observed (Fig. 2a) the control run (Fig. 2b) shows some similarity in horizontal pattern, but with a displacement for the northeast part of the domain. This behavior suggests that the simulated field, by the control run, is ahead of the observation. The experiment BMJn90 (Fig. 2c) removed the precipitation over the South-

west of São Paulo and expanded the areas with precipitation in the South of Minas Gerais. The increase in the threshold for saturation of the grid point from which the microphysics scheme triggers precipitation, through the experiment RHgrd1.1 (Fig. 2d) did not alter the spatial pattern of precipitation but reduced the peaks in areas of higher intensity (Fig. 2g), as expected since the purpose of the experiment was to constrain the formation of clouds drops and, consequently, the precipitation. The experiment that increases the ice crystal velocity (Fig. 2f) increases the amount of precipitation while its reduction (Fig. 2e) decreases the amount and slightly reduces the covered area

Conclusions

Changes related to the experiment with variation in the terminal velocity of the ice crystal were almost insignificant, mainly, in relation to the spatial distribution pattern of the precipitation. The experiment RHgrd1.1 was able to change the amount of precipitation simulated by the model and failed to simulate the positioning of precipitation bands. On the other hand, BMJn90 modified the spatial pattern of precipitation and increased the precipitation area in some places. None of the experiments adequately simulated the positioning of the observed.

References

Betts AK, and Miller MJ (1986): A new convective adjustment scheme. Part II: Single column tests using GATE wave, BOMEX and arctic air-mass data sets. Quart. J. Roy. Meteor. Soc., **112**., 693-709.

Ferrier BS, Lin Y, Black T, Rogers E, DiMego G (2002) Implementationof a new grid-scale cloud and precipitation scheme in theNCEP Eta model. In: 15th Conference on numerical weather prediction, Amer. Meteor. Soc., San Antonio, TX, 280–283 (preprint)

Mesinger F (1984). A blocking technique for representation of mountains in atmospheric models. Riv. Meteor. Aeronautica, **44**, 195-202.

Overview of the KIAPS's next generation global model (KIM; Korea Integrated Model)

Young C. Kwon, Song-You Hong, and KIAPS scientists
Korea Institute of Atmospheric Prediction Systems
(yc.kwon@kiaps.org)

Introduction

The purpose of the nine year project of Korea Institute of Atmospheric Prediction Systems (KIAPS) is developing a next generation global model for operational use at the Korea Meteorological Administration (KMA). After conducting basic research and development in the first stage of the project, KIAPS configured the beta-version NWP system from data assimilation to post-pocess (KIM: Korea Integrated Model). KIAPS has been running KIM on the semi-realtime basis since July 2015. Since the start of semi-realtime run, the performance of KIM has improved significantly due to continuous update of the model.

KIM's dynamic core consists of non-hydrostatic governing equation set on cubed sphere projection with spectral element method. Physics packages are developed based on Weather Research and Forecasting (WRF) model and Global-Regional Integrated Model system (GRIMS) physics packages. KIAPS scientists have implemented several vital aspects of physics parameterizations such as non-orographic gravity wave drag, gray-zone convection, top-down mixing method in PBL, prognostic cloudiness, and radiation-cloud interactions. The KIM is a self-cycled 4DEnVAR data assimilation system with its own data acquisition and quality control. In this talk, the performance of the KIM will be presented on top of the brief overview of KIM in terms of dynamics, physics, and data assimilation system.

Dynamic Core

Dynamic core of a NWP model consists of temporal and spatial (horizontal and vertical) discretization of governing equations; projection of spherical shape earth; and numerical diffusion. At the early stage, KIAPS has selected cubed-sphere grid system with spectral element method in horizontal direction and sigma-p vertical coordinates with finite difference method. The governing equations are non-hydrostatic flux-type equations, and numerical diffusion is 6^{th} order split-explicit Newtonian method. Different from many operational global models of using implicit method, time integration is explicit Runge-Kutta 3^{rd} order method with separate treatment of fast moving waves.

The advantages of cubed-sphere are avoiding pole singularity due to better

equidistance and high scalability due to smaller communication overhead. However, numerical noise can occur along the edges of cube and spectral element method on cubed-sphere grid is computationally expensive (Hong et al, 2018, Choi and Hong, 2016).

Fig, 2.1. Example of Cubed-sphere grid system used in KIM

Since the prototype version of KIM's dynamic core was designed successfully, several upgrades have been made. For example, higher order horizontal diffusion with explicit-split method (4th to 6th order), finer horizontal resolution (NE120 to NE240 ~12km), and higher model top level (50km to 80km). Recent plan of upgrading dynamic core are mostly focused on improving computational efficiency in order to accommo-date operational time requirement. Some of them are converting dynamical calculations over entire points to unique point as shown in Fig. 2.2, and reducing the order of basis function from 4th to 3rd. Overall, it is expected the computational time will be reduced to about 50% with these changes.

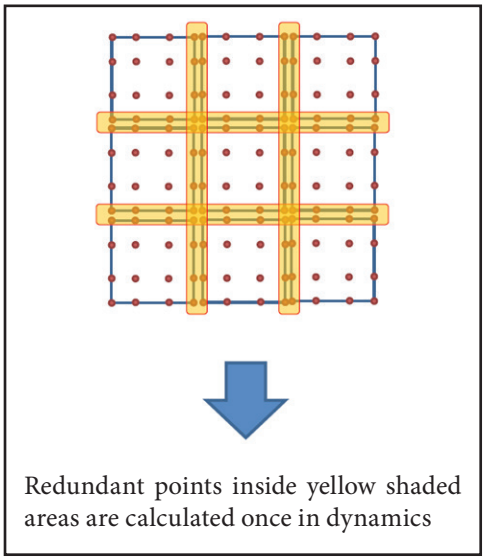

Fig. 2.2 Grid points configuration change

Physics

Although most of the physics schemes of KIM is originated from other community models such as WRF model and GRIMS, they are greatly revised by KIAPS scientists. The emphases of upgrading physics schemes are minimizing artificial tuning, keeping consistency between individual scheme, and adding scale-aware capability.

For example, one of the revisions of the deep convection parameterization scheme (Simplified Arakawa-Schubert scheme, SAS) has been added scale-aware function (Kwon and Hong, 2017). The main concept of the new scale-aware SAS is the magnitude of subgrid scale convective parameterization becomes smoothly weakens with smaller horizontal grid size and weaker grid scale vertical velocity. The test shows that the precipitation simulations better agree with observation with the new scheme as shown in Fig. 3.1.

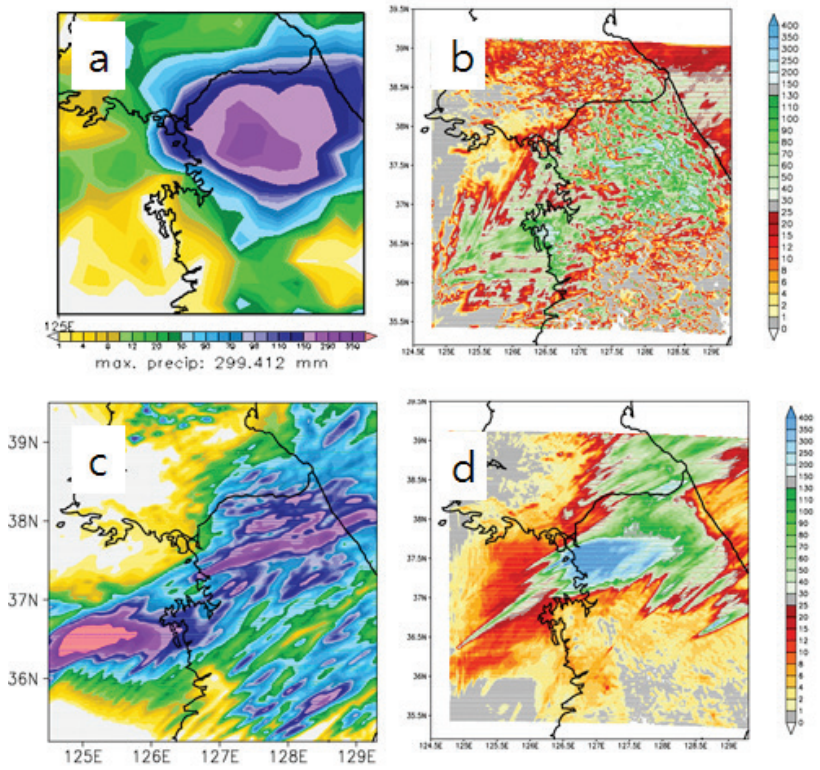

Fig. 3.1. 24hour accumulated precipitation amount at 12UTC 27th July 2011, where a) TMPA observation, b) original SAS, c) no CPS and d) new SAS.

Data Assimilation

KIAPS data assimilation team has built the first fully functional data assimilation system on the cubed-sphere grid system. While three dimensional data assimilation system was implemented initially, the major upgrade was made to the hybrid four dimensional variational-localized ensemble system (4DEnVar) which was implemented at March of 2017. Since then, many aspects of data assimilation systems are upgraded such as localization of the ensemble, typhoon bogusing, vertical and horizontal thinning method, and other technical/scientific aspects. Currently, the weight of variational and ensemble analysis increment is 0.7 and 0.3 respectively. However, the skills of ensemble analysis improves with time, the plan is to increase the weight of ensemble method (Kwon et al, 2018).

Although the amount of observation data assimilated to KIM is very limited at the early stage, most of the data which are into the operational NWP models are used in KIM analysis. Table. 4.1 summarized the data assimilated to KIM compare to the operational global model at Korea Meteorological Administration (KMA).

Fig. 4.1 shows the analysis field of 500hPa geopotential height of KIM, Unified

Table. 4.1 Comparison of data assimilate to the KIAPS and KMA global model

Observation type		KMA	KIAPS	Observation type		KMA	KIAPS
1	SONDE	○	○	9	IASI	○	○
2	SURFACE	○	○	10	CrIS	○	○
3	AIRCRAFT	○	○	11	ATMS	○	○
4	SCATWIND	○	○	12	AMV	○	○
5	HIRS	○	×	13	GPS-RO	○	○
6	AMSU-A	○	○	14	CSR	○	○
7	MHS	○	○	15	SSMIS	×	Testing
8	AIRS	○	×	16	TC bogus	○	○

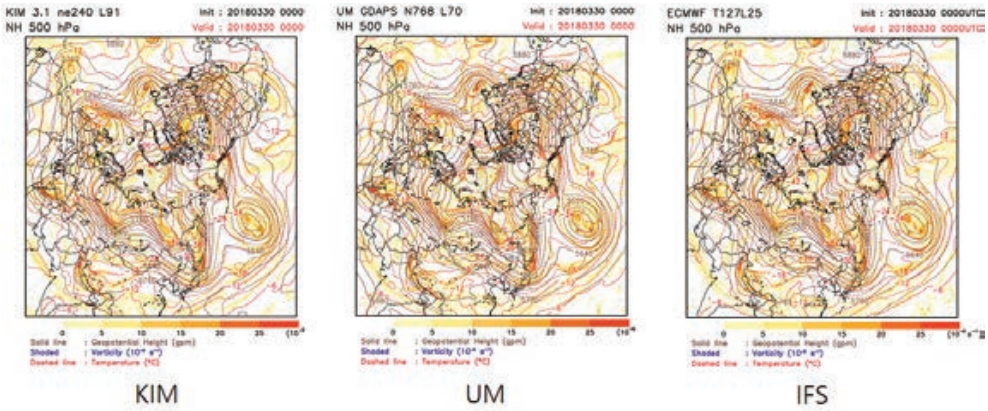

Fig. 4.1 Analysis field of 500hPa geopotential height for KIM, UM and IFS over Northern Hemisphere

Model from UK Met Office and IFS from ECMWF. As can be seen in the pictures, the main feature of the systems are well represented in all three analyses.

Framework and Verification Results

In the operational environment, the efficiency is as important as the accuracy of the model because the model output are required to deliver to the forecasters within given time frame. Model Framework consists of optimization, parallelization and other necessary tools to run the model effectively. The scientists of KIAPS have developed several unique tools for cubed sphere grid system and are currently developing other useful software. For example, a bilinear interpolation method that can be applied between any unstructured grids, neighbor grids searching algorithm on the cubed sphere and optimized IO system are developed (e.g., Kim et al, 2018). In addition, flexible KIM system which can be run many

different high performance computers is currently designed at KIAPS, which is called PyMIP – Python-based Machine Independent Platform (Fig. 5.1).

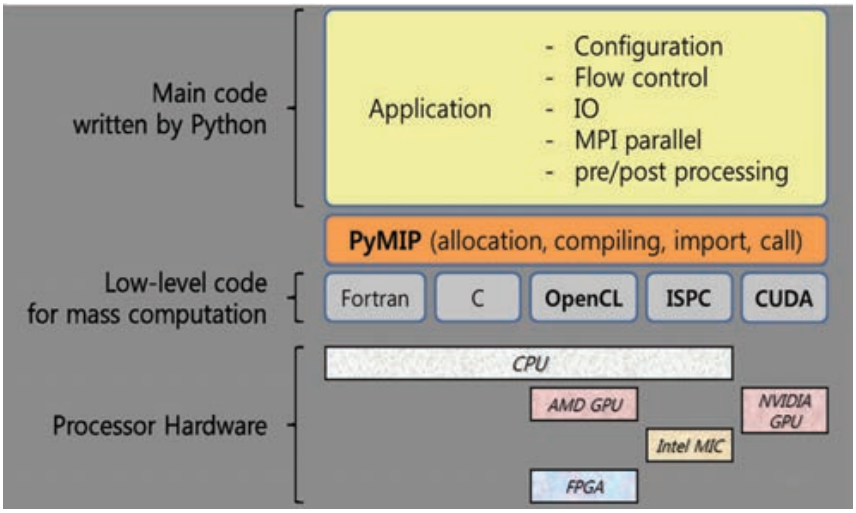

Fig. 5.1 Schematics of multi-platform KIM

The performance of KIM has been monitored since KIM was operated semi-realtime basis from July 2015. The time series of the anomaly correlations of 500hPa geopotential height of KIM and UM up to April 2018 are shown in Fig. 5.2. At Jan 2018, anomaly correlation of KIM almost reached that of UM, however the skill dropped sharply after that. KIAPS staff found that there is a bug in the data assimilation of mean sea level pressure, and fixed the problem in the next version of KIM (2018 July).

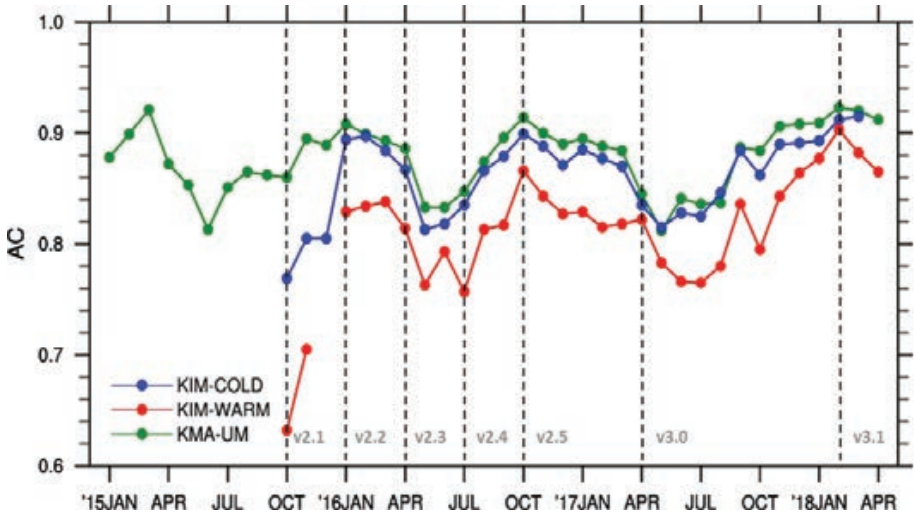

Fig. 5.2 500hPa geopotential height anomaly correlations of UM and KIM over Northern Hemisphere

Summary

Since KIAPS began 9 year project to develop a next generation global model for KMA's operational purpose at 2011, KIAPS is on the verge of finishing the initial version of the operational modeling system. Although the overall prediction skill of KIM is a little behind the skill of the current KMA operational global model (UM from UK Met Office), KIAPS keeps updating all the components of the system including physics, dynamics and data assimilation. KIM consists of non-hydrostatic dynamic core on cubed sphere grid, state-of-art physics scheme and four dimensional variation-ensemble data assimilation system built on cubed sphere. In addition, optimization of model system has been performed to fit the time window of operational set up, such as IO, parallelization, interpolation, and so on. To accommodate the developing trend of high performance computing system, KIAPS staffs enable KIM codes to operate in different architectures. It is planned for KIM to be an official operational global model at KMA om year 2020.

References

Choi, S.-J and S.-Y. Hong (2016) A global non-hydrostatic dynamic core using the spectral element method on a cubed sphere grid, *Asia-Pac. J. Atmos. Sci.*, **52**, 291-307

Hong, S.-Y and co-authors (2018) The Korea Integrated Model (KIM) system for global weather forecasting, *Asia-Pac. J. Atmos. Sci.*, **54(s)**, 267-292

Kim, J., Y. C. Kwon and T.-H. Kim, (2018), A scalable high-performance I/O system for a numerical weather forecast model on the cubed-sphere grid, *Asia-Pac. J. Atmos. Sci.*, **54(s)**, 403-412

Kwon, Y. C., and S.-Y. Hong (2017) A mass-flux cumulus parameterization scheme across gray-zone resolutions, *Mon. Wea. Rev.*, **145**, 583-598

Kwon, I.-H. and coauthors (2018) Development of an operational hybrid data assimilation system at KIAPS, *Asia-Pac. J. Atmos. Sci.*, **54(s)**, 203-318

Development and evaluation of Global Eta Framework (GEF) model at medium and seasonal ranges

Dragan Latinović[1], Chou Sin Chan[1], Miodrag Rančić[2], Jonas Tamaoki[1], Gustavo Sueiro[1], Jorge Gomes[1] and André Lyra[1]

[1] CPTEC/INPE, Cachoeira Paulista, SP, Brazil (dragan.latinovic@inpe.br)
[2] IMSG at EMC/NCEP/NOAA, College Park, MD, USA

Introduction

Several high-resolution global atmospheric models are in use today in many institutions around the world, with applications ranging from experimental science to operational forecasting. With the advances achieved in computer technology, there is an increasing tendency to unify climate models with global weather prediction models. New technologies such as variable-resolution mean that parts of the globe can now be simulated at extremely high resolutions. The concept of a unified or seamless framework for weather and climate prediction, that attracted a lot of attention in the last few years (Hurrell et al., 2009; Brunet et al., 2010; Shapiro et al., 2010; Nobre et al., 2010; Hazeleger et al., 2010; Senior et al., 2011) was the motivation to explore the potential of Global Eta Framework model (GEF) (Zhang and Rančić, 2007) to run at high resolution in weather and climate simulations. As an early stage of going in that direction, GEF is configured and evaluated at 25-km horizontal resolution for the seasonal integrations and 8-km horizontal resolution for the medium-range integrations. The main objective of this research is to evaluate the model skill in simulating the onset of the rainy season in seasonal runs over the region of Western-Central Brazil (WCB), and in simulating the extreme precipitation events in the medium-range simulations over the Amazon region.

Model

GEF is a global atmospheric model, based on general curvilinear coordinates, capable of running on various rectangular spherical grids. In this study, the model uses a cubed-sphere grid topology, whose symmetry and uniformity enable a highly scalable and efficient performance. A specific version of the cubed-sphere used in this study provides an equal-area grid topology (with exception of three grid boxes around vertices) without angular discontinuities across the edges (Purser and Rančić, 2011; Purser et al., 2014; Rančić et al., 2017) which characterizes the gnomonic cubed-sphere, originally suggested for modeling of the atmosphere by Sadourny (1972). GEF is created as a combination of the technique of quasi-uniform gridding of the sphere and the numerical structure of the regional Eta model (Mesinger et al., 1988; Janjic, 1990; Janjic, 1994; Black, 1994;

Chou et al 2002, 2012; Mesinger et al., 2002; Pesquero et al., 2010; Mesinger et al., 2012; Lyra et al., 2017; Mesinger and Veljovic, 2017) therefore it represents a unique global version of the regional Eta model. Six regional models, interconnected through the cubed-sphere framework are integrated simultaneously, one on each side of the cube, to provide a global coverage and to create the global model – GEF.

Seasonal range integrations

A comparative assessment of simulated and observed seasonal conditions for the trimester September-October-November (SON) of the years 2011 and 2013 is performed in this chapter, with emphasis on the evaluation of the model skill to simulate the onset of the rainy season in the region of WCB (20°S-10°S, 60°W-50°W) (Fig. 3.2). For that purpose, the methods based on pentads of precipitation (Marengo et al., 2001) and OLR (Kousky, 1988) were applied. The rainy seasons of both selected years ended with extreme floods in the Amazon region, which is the motivation to use them in this study. A total of 10 seasonal integrations were performed, for the range of approximately 4 months, creating ensembles of 5 members for each season.

Table 3.1: Spatial correlations of daily mean global simulations and CMORPH observations for precipitation (mm day-1) and the NCEP reanalyses for other variables, for the SON of 2011 and 2013.

variables / trimester	200-hPa wind ($m\ s^{-1}$)	500-hPa geopotential height (hPa)	850-hPa temperature (°C)	850-hPa wind ($m\ s^{-1}$)	MSLP (hPa)	precipitation ($mm\ day^{-1}$)
SON 2011	0.89	0.99	0.98	0.86	0.89	0.64
SON 2013	0.88	0.99	0.98	0.85	0.88	0.64

Table 3.1 shows the high values of spatial correlation, 0.99 for 500-hPa geopotential height and 0.98 for 850-hPa temperature for both years. The mean sea-level pressure (MSLP), together with 200-hPa wind, holds the third position in spatial correlation coefficients, when compared with all other analyzed fields. The spatial correlations for both MSLP and 200-hPa wind are 0.89 and 0.88 for the years 2011 and 2013. The 850-hPa wind correlations are 0.86 and 0.85, for 2011 and 2013, respectively. Spatial correlations of precipitation of 0.64 for both years can be considered reasonably good. Despite the lowest correlation, model precipitation patterns show reasonable agreement with the high resolution CMORPH (CPC MORPHing technique, Joyce et al., 2004) observations (Figure 3.1). The Intertropical Convergence Zone (ITCZ) is correctly positioned across the Pacific Ocean and over the Atlantic and Indian Oceans and the Maritime continent. However, precipitation rate is underestimated over central Pacific, over tropical South America and Africa and overestimated over Central America, Indian Ocean and over the western Pacific. The South Pacific Convergence Zone (SPCZ) that extends from the equatorial west Pacific southeastward across the south Pa-

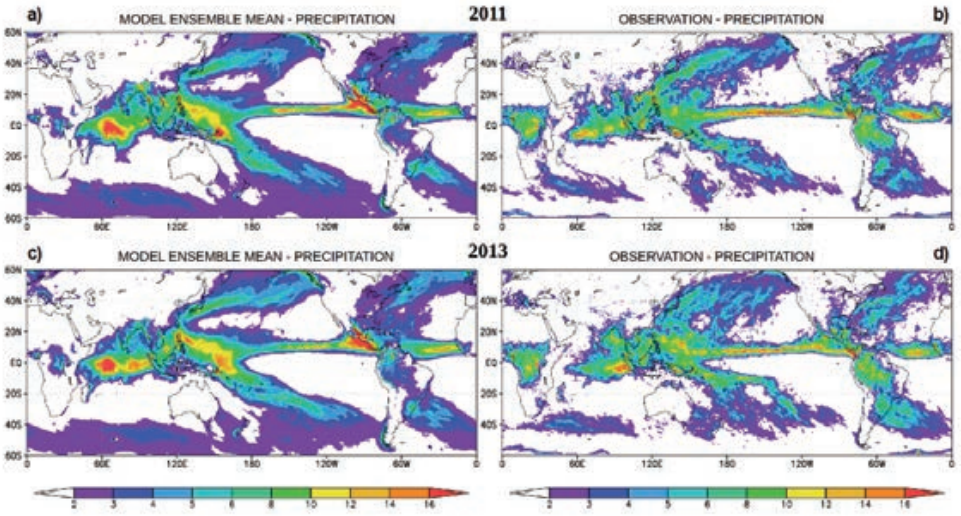

Figure 3.1: 2011 and 2013 SON global ensemble mean precipitation (mm day-1); GEF simulations (on the left,((a) and (c))) and observed precipitation (mm day-1) from CMORPH (on the right, ((b) and (d))). The top row shows precipitation (mm day-1) in 2011 and the bottom row shows precipitation (mm day-1) in 2013.

cific Ocean is correctly positioned. The simulated precipitation rate is also comparable to observations precipitation intensity. Similarly, the precipitation band over South Atlantic that extends from South America also has the quantities comparable to the observations. The weak precipitation areas in the southern hemisphere mid-latitudes are slightly overestimated by the model, while in the northern hemisphere mid-latitudes, the precipitation maxima along and off the eastern coasts of the continents are mostly well represented both in position and intensity. The simulations reproduce the precipitation minima in the mid-latitudes, which correspond to the positions of subtropical highs and the desert regions over the continents along the latitudes of 20°. Model precipitation pattern over South America reproduces the initial phase of onset of the rainy season which is indicated by the spatial distribution of precipitation, although the intensity of precipitation is clearly underestimated, especially over the Amazon region and the La Plata river basin. Global models generally show dry bias in these two regions (Yin et al., 2012).

Figure 3.2: Study area to define the rainy season onset, Western-Central Brazil (WCB), 10°S–20°S/60°W–50°W.

Time-longitude daily mean precipitation, averaged over 20°S-10°S for the period SON 2011 and 2013, is presented in Figure 3.3. The model simulates some pre-onset episodes of rain in WCB region in September, with the first intense continuous precipitation occurring in the period 23-28 September (approximately pentad 54), while in the observations the onset is identified in the period 26 September-2 October (approximately pentad 55). Lower charts show the ensemble mean simulated by the model for 2013 on the left and observed data on the right, and show relatively similar pattern as in 2011. The difference is that model produces little rain in the first 20 days of September, simulating some weak rain only at the beginning of the last 10 days of September. More intense rain is simulated only in the eastern part of WCB region in the period 1-6 October (approximately pentad 56). Observed data show some rainy episodes in September with more intense continuous rain occurring in the period 28 September-2 October (approximately pentad 55). Precipitation is notably more intense in observations for both years. More figures and details about seasonal range integrations are presented in Latinović et al. (2018).

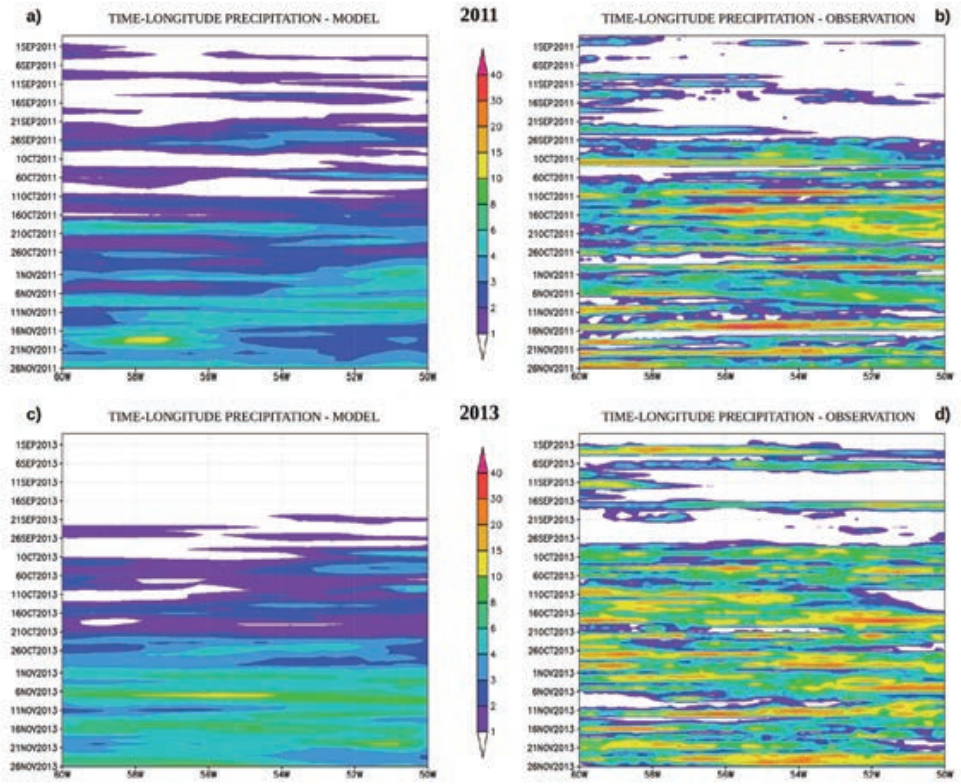

Figure 3.3: Time-longitude daily precipitation (mm day-1) averaged over 20°S–10°S for the period between 9 August-26 November (pentads 49-66) of 2011 (top row) and 2013 (bottom row). Simulated precipitation (mm day-1) is on the left ((a) and (c)) and observed precipitation is on the right ((b) and (d)).

Medium range integrations

Extremes of precipitation are not well represented by global models. Extreme events of short duration are considered some of the most impacting (Marengo, 2009). These events in the form of large amounts of rainfall in a short period of time are very frequent in Manaus, AM. Over the past 10 years, the Amazon basin has experienced frequent floods (Espinoza et al., 2012; Marengo et al., 2012; Satyamurty et al., 2012) that directly impact the lives of its people.

A newly developed and configured high-resolution, 8-km, hydrostatic version of the GEF model is integrated for the period of 10 days with 22 different sets of initial conditions with some results presented in this chapter. The model skill to simulate various atmospheric fields is assessed in a comparative analysis of simulated fields against reanalyses and observations (figures not shown here). One selected case with intense precipitation over the city of Manaus, AM (21st April 2013) is also presented with the objective to evaluate the model skill to simulate the events of extreme precipitation in tropical environment with lead times of 24, 48 and 72 hours. More details, that include analysis of other atmospheric fields, the other cases of extreme precipitation, together with the model assessment using some continuous and cate-

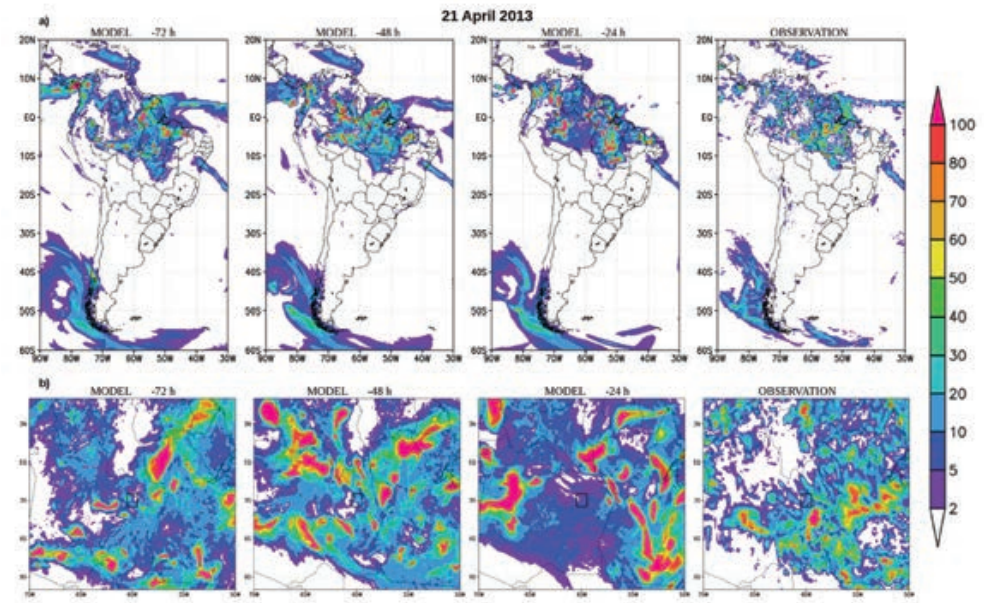

Figure 4.1: Daily accumulated precipitation (mm day^{-1}) for 0000 UTC 21 April 2013 for: (a) South America (60°S – 20°N, 90°W – 30°W) and (b) Central Amazon (10°S – 5°N, 70°W – 50°W). Plots from left to right represent the simulations by GEF with the lead time of: (a) 72 h, (b) 48 h, (c) 24 h and (d) corresponding CMORPH precipitation data, respectively. The black square in the middle of the lower plots (3.5°S – 2.5°S, 60.5°W – 59.5°W) represents the area that surrounds the city of Manaus (3.1190°S, 60.0217°W), which is positioned approximately in the centre of that square.

gorical statistical scores can be found in Latinović (2018). The period between 20 and 22 April 2013 was characterized by large areas of convective instability that caused heavy rainfall in Brazilian states of Amazonas and Pará. A zone of moisture present in the previous days (17 and 18 of April 2018, figures not shown) propagated in the northwest-southeast direction reaching the nortwesternmost areas of the states of Amazonas and Pará. The moisture convergence zone remained over the area for a few days. This moisture convergence and the warm air temperature lead to vertical movements and formation of the deep convection and precipitation. The Brazilian National Institute of Meteorology (INMET) registered precipitation of 117.4 mm on 21 of April and 140 mm on 22 of April (measurements are taken at 8 AM, local time) in the city of Manaus. The measured amount of 140 mm day^{-1} on 22 of April 2013 was the heaviest registered in Manaus in that year. The total of 257.4 mm day^{-1} accumulated in 48 hours has almost reached the average monthly amount of 311.2 mm day^{-1}. Figure 4.1 shows 24-h accumulated precipitation on 20 April 2013 0000 UTC over South America (upper plots) and over the Central Amazon, 10° S – 5° N, 70° W - 50° W, for the simulations with lead time of 72 h, 48 h, and 24 h and observation. The area with intense precipitation occurred over the northern part of the continent, mostly over the Amazon region and Brazilian Northeast. The band of precipitation that spreads approximately between the equator and 5° N over the Atlantic Ocean corresponds to the ITCZ and narrow band of precipitation that extends from the coast of Brazilian state of Bahia towards southeast corresponds to the part of the weakening moisture convergence zone, which was active in the region in the previous days. In all lead times, the model simulated well the position of precipitation areas in tropics, changing mostly the intensity of the precipitation maxima, giving more locally intense precipitation in 24 h lead time, which is clear in the plots of the Central Amazon. The model simulates rain of different intensity inside in Manaus city in all lead times, between 5-20 mm day^{-1} in the centre of the city and over 100 mm day^{-1} near the borders of the city in the 48-h lead time. However, CMORPH estimate shows less precipitation than observed by INMET station data, with difference of up to 50 mm day^{-1} between the two datasets. That difference in observed data might be attributed to the different time of measurements and to the technique used by the CMORPH data set to estimate precipitation.

Conclusions

The ability of the model to simulate the onset of the rainy season in WCB is best demonstrated in the Figure 3.3, which shows the time-longitude daily averaged precipitation over the latitudes 20°S-10°S. It is clearly shown that with the difference of couple of days (earlier in 2011, and later in 2013) when compared against observed data, the model shows transition of precipitation regime from dry to wet, approximately at the end of September, beginning of October. Precipitation pattern changes and more intense precipitation starts to occur after that date, although still significantly less intense than observed.

The simulations of precipitation over South America with the lead times of 24, 48 and 72 hours are compared against appropriate observations with objective to evaluate the model skill to simulate 8 events of extreme precipitation over the city of Manaus. The areas with precipitation over South America are well simulated by the model, which is in agreement with conclusions obtained from categorical analysis (not shown here). In the terms of intensity, the model performed well in extratropical regions while the precipitation in tropical regions was mostly underestimated. Finally, the model simulated rain for Manaus in almost every presented simulation (only one case presented here), with underestimated values in most of the cases. However, in the region of Central Amazon, the model simulates well the areas with precipitation, but also shows low skill in simulation of the positions of precipitation maxima.

The simulations of the model at 25-km horizontal resolution, with time step of 40 s, 38 vertical levels and the model top at 25 hPa were performed with relatively modest use of computational resources, using 600 processor cores, where 1 day of simulation was performed in approximately 6 min. On the other hand, the simulations of the model at 8-km horizontal resolution, with time step of 10 s, 38 vertical levels and the model top at 25 hPa were performed using 1176 processor cores, where 1 day of simulation was performed in approximately 1 h 20 min. These results demonstrate computational efficiency of both configurations of the model, especially when compared with current global atmospheric model, used for weather forecasts at CPTEC (BAM, Figueroa et al., 2016), that has 64 vertical levels, runs at 20-km horizontal resolution, uses 4320 processor cores and takes 2 h 15 min for a 1-day forecast.

BAM runs at 20-km horizontal resolution, while the global atmospheric operational model used for long-term simulations (AGCM, latest results presented in Cavalcanti and Raia (2017)) runs at approximately 200-km horizontal resolution. Therefore, the results shown in this research present a contribution for the centre, also in the terms of improvement in horizontal resolution. However, even if GEF performed reasonably well, both in medium-range and seasonal scales, the presented results indicated that the further improvements are needed. In the model configured at 25-km horizontal resolution, underestimate of precipitation over tropical continental regions, particularly over South America remains one of the main issues, together with the overestimate presented in analysis of OLR (figures not shown here). The model configured at 8-km horizontal resolution also showed difficulties in simulation of precipitation, where the main issues are related with continuous increase of global mean precipitation after day 5 and inappropriate distribution of the intensity of precipitation. The implementation of RRTMG radiation parameterization scheme will hopefully improve the simulation of OLR and favor the better representation of radiation and precipitation. Also, further adjustments in parameterization scheme for convection are expected to contribute in improvement in simulation of precipitation. Presented results show that GEF is capable of running at high resolution in weather and climate

simulations and providing reasonable results. For the purpose of development of the concept of a unified or seamless framework for weather and climate prediction, further development and tests are needed. Incorporation of the refined vertical coordinate that uses "sloping steps" (Mesinger et al., 2012) and development of the nonhydrostatic version of GEF remain as a future task.

References

Black TL. 1994. The new NMC mesoscale Eta model: Description and forecast examples. *Weather and Forecasting* **9**: 265–278.

Brunet G, Shapiro M, Hoskins D, Moncrieff M, Dole R, Kiladis GN, Kirtman B, Lorenc A, Mills B, Morss R, Polavarapu S, Rogers D, Schaake J, Shukla J. 2010. Collaboration of the weather and climate communities to advance sub-seasonal to seasonal prediction. *Bulletin of the American Meteorological Society*, v. **91**, p. 397–1406

Cavalcanti IFA, Raia A. 2017. *Lifecycle of South American Monsoon System simulated by CPTEC/INPE AGCM. Int. J. Climatol.* **37***: S1 878–896. doi: 10.1002/joc.5044.*

Chou SC, Marengo JA, Lyra A, Sueiro G, Pesquero J, Alves LM, Kay G, Betts R, Chagas D, Gomes JL, Bustamante J, Tavares P. 2012. Downscaling of South America present climate driven by 4-member HadCM3 runs. *Clim. Dynam.* **38**: 635–653. https://doi.org/10.1007/s00382-011-1002-8.

Espinoza JC, Ronchail J, Frappart F, Lavado W, Santini W, Guyot JL. 2012. The major floods in the Amazonas river and tributaries (Western Amazon Basin) during the 1970-2012 period: a focus on the 2012 flood. *Journal of Hydrology*, v. **14**, p. 1000- 1008.

Figueroa SN, Bonatti JP, Kubota PY, Grell GA, Morrison H, Barros SRM, Fernandez JPR, Ramirez E, Siqueira L, Luzia G, Silva J, Silva JR, Pendaharkar J, Capistrano VB, Alvim DS, Enoré DP, Diniz FLR, Satyamurty P, Cavalcanti IFA, Nobre P, Barbosa HMJ, Mendes CL, Panetta J. 2016. *The Brazilian global atmospheric model (BAM): performance for tropical rainfall forecasting and sensitivity to convective scheme and horizontal resolution. Weather Forecast, v.* **31***, p. 1547–1572.*

Hazeleger W, Severijns C, Semmler T, Stefanescu S, Yang S, Wang X, Wyser K, Dutra E, Baldasano JM, Bintanja R, Bougeault P, Caballero R, Ekman AML, Christensen JH, Van den Hurk B, Jimenez P, Jones C, Kallbeg P, Koenigk T, McGrath R, Miranda P, van Noije T, Palmer T, Parodi JA, Schmith T, Seltn F, Storelvmo T, Sterl A, Tapamo H, Vancoppenolle M, Viterbo P, Willén U. 2010. EC-Earth: A seamless Earth-system prediction approach in action. *Bulletin of the American Meteorological Society,* v. **91**, p. 1357-1363.

Hurrell JW, Meehl GA, Bader D, Delworth T, Kirtman B, Wielicki B. 2009. A unified modeling approach to climate system prediction. *Bulletin of the American Meteorological Society*, v. **90**, p. 1819–1832.

Janjic ZI. 1990. The step-mountain coordinate: physical package. *Mon. Weather Rev.* **118**: 1429–1443.

Janjic ZI. 1994. The step-mountain eta coordinate model: Further develop-

ments of the convection, viscous sublayer, and turbulence closure schemes. *Mon. Weather Rev.* **122**: 927–945.

Joyce RJ, Janowiak JE, Arkin PA, Xie P. 2004. CMORPH: A Method That Produces Global Precipitation Estimates From Data At High Spatial And Temporal Resolution. *J. Hydrometeor.* **5**: 487-503.

Kousky VE. 1988. Pentad outgoing longwave radiation climatology for the South American sector. *Revista Brasileira de Meteorologia* **3**: 217–231.

Latinović, D. : Development and evaluation of Global Eta Framework (GEF) model at medium and seasonal ranges, PhD thesis, available at http://mtc-m21c.sid.inpe.br/col/sid.inpe.br/mtc-m21c/2018/03.15.18.01/doc/publicacao.pdf (last access: 17 August 2018), 2018.

Latinović, D., Chou, S. C., Rančić, M., Sueiro, G., and Lyra, A.: Seasonal climate and the onset of the rainy season in Western-Central Brazil simulated by Global Eta Framework model. *International Journal of Climatology*, 2018 (accepted)

Lyra A, Tavares P, Chou SC, Sueiro G, Dereczynski C, Sondermann M, Silva A, Marengo J, Giarolla A. 2017. Climate change projections over three metropolitan regions in Southeast Brazil using the non-hydrostatic Eta regional climate model at 5-km resolution. *Theor. Appl. Climatol.* https://doi.org/10.1007/s00704-017-2067-z.

Marengo JA. 2009. Impactos de extremos relacionados com o tempo e o clima: impactos sociais e econômicos. *Boletim do Grupo de Pesquisa em Mudanças Climáticas*, v. **8**, p. 1-5.

Marengo JA, Tomasella J, Soares WR. 2012. Extreme climate events in the Amazon Basin. *Theoretical and Applied Climatology*, v. **107**, p. 73-85. Available at: http://dx.doi.org/10.1007/s00704-011-0465-1.

Marengo J, Liebmann B, Kousky VE, Filizola N, Wainer I. 2001. On the onset and end of the rainy season in the Brazilian Amazon Basin. *Journal of Climate* **14**: 833–852.

Mesinger F, Jovic D. 2002. The Eta slope adjustment: Contender for an optimal steepening in a piecewise-linear advection scheme? Comparison tests. NOAA/NCEP Office Note 439 available at: http://www.emc.ncep.noaa.gov/officenotes/newernotes/on439.pdf (last access: 26 November 2017).

Mesinger F, Veljovic K. 2017. Eta vs sigma: Review of past results, Gallus–Klemp test, and large-scale wind skill in ensemble experiments. *Meteorol. Atmos. Phys.* https://doi.org/10.1007/s00703-016-0496-3.

Mesinger F, Janjic ZI, Ničković S, Gavrilov D, Deaven DG. 1988. The step mountain coordinate: Model description and performance for cases of Alpine cyclogenesis and for a case of an Appalachian redevelopment. *Mon. Weather Rev.* **116**: 1493–1518.

Mesinger F, Chou SC, Gomes JL, Jovic D, Bastos P, Bustamante JF, Lazic L, Lyra AA, Morelli S, Ristic I, Veljovic K. 2012. An upgraded version of the Eta model. *Meteorol. Atmos. Phys.* **116**: 63–79. https://doi.org/10.1007/s00703-012-0182-z.

Nobre C, Brasseur GP, Shapiro MA, Lahsen M, Brunet G, Busalacchi AJ, Hibbard K, Seitzinger S, Noone K,

Ometto JP. 2010. Addressing the complexity of the Earth system. *Bulletin of the American Meteorological Society*, v. **91**, p. 1389–1396.

Pesquero JF, Chou SC, Nobre CA, Marengo JA. 2010. Climate downscaling over South America for 1961–1970 using the Eta Model. *Theor. Appl. Climatol.* **99**: 75–93. https://doi.org/10.1007/s00704-009-0123-z.

Purser RJ, Rančić M. 2011. A standardized procedure for the derivation of smooth and partially overset grids on the sphere, associated with polyhedra that admit regular griddings of their surfaces. Part I: Mathematical principles of classification and construction. NOAA/NCEP Office Note 467, available at: http://www.emc.ncep.noaa.gov/officenotes/newernotes/on467.pdf (last access: 26 November 2017).

Purser RJ, Rančić M, Jović D, Latinović D. 2014. Two strategies for the mitigation of coordinate singularities of a spherical polyhedral grid, Presentation from 2014 PDEs workshop, Boulder, CO, USA, available at: http://www.cgd.ucar.edu/events/20140407/Presentations-Posters/Purser.pdf (last access: 26 November 2017).

Rančić M, Purser RJ, Jović D, Vasić R, Black T. 2017. A nonhydrostatic multiscale model on the uniform Jacobian cubed sphere, *Mon. Weather Rev.* https://doi.org/10.1175/MWR-D-16-0178.1.

Sadourny R. 1972. Conservative finite-differencing approximations of the primitive equations on quasi-uniform spherical grids. *Mon. Weather Rev.* **22**: 1107–1115.

Satyamurty P, Da Costa CP, Manzi AO, Candido LA. 2013. A quick look at the 2012 record flood in the Amazon Basin. *Geography Research Letter*, v. **40**, p. 1-6, available at: http://dx.doi.org/10.1002/grl.50245.

Senior CA, Arribas A, Brown AR, Cullen MJP, Johns TC, Martin GM, Milton SF, Webster S, Williams KD. 2011. Synergies between numerical weather prediction and general circulation climate models. In: Donner L, Schubert W, Somerville R (Eds.). *The development of atmospheric general circulation models*. Cambridge: Cambridge University Press, p. 76–116.

Shapiro M, Shukla J, Brunet G, Nobre C, Beland M, Dole R, Trenberth K, Anthes R, Asrar G, Barrie L, Bougeault P, Brasseur G, Burridge D, Busalacchi A, Caughey J, Chen DL, Church J, Enomoto T, Hoskins B, Hov O, Laing A, Letreut H, Marotzke J, McBean G, Meehl G, Miller M, Mills B.; Mitchell J, Moncrieff M, Nakazawa T, Olafsson H, Palmer T, Parsons D, Rogers D, Simmon A, Troccoli A, Toth Z, Uccellini L, Velden C, Wallace JM. 2010. An earth-system prediction initiative for the twenty-first century. *Bulletin of the American Meteorological Society,* v. **91**, p. 1377–1388.

Yin L, Fu R, Shevliakova E, Dickinson RE. 2013. How well can CMIP5 simulate precipitation and its controlling processes over tropical South America?. *Climate Dynamics* **41** (11-12): 3127–3143. Zhang H, Rančić M. 2007. A global Eta model on quasi-uniform grids. *Q. J. Roy. Meteorol. Soc.* **133**: 517–528.

Cut-cell Eta: Some history, and lessons from its present skill

Fedor Mesinger[1] and Katarina Veljovic[2]

[1] Serbian Academy of Sciences and Arts, Belgrade, Serbia
(fedor.mesinger@gmail.com)
[2] Institute of Meteorology, University of Belgrade, Belgrade, Serbia
(katarina@ff.bg.ac.rs)

Some history

The history of the Eta model goes back to an effort started at the University of Belgrade, then Yugoslavia, in the early seventies. For some detail, we shall here include excerpts from Mesinger 2004), which can be consulted for still more detail.

"Design of the very first Eta ancestor code, the dynamical core in today's terminology, was done with the aim to follow the Arakawa approach. This first code I wrote mostly during the one-month academic break January-February 1973. This was the time just after the pioneering efforts of Arakawa during the sixties and the beginning of seventies, at the dawn of the atmospheric primitive equation modeling. For example, and quite incidentally, precisely during that same time period, on 7 February 1973 (NWS 1973), for the first time forecast boundary conditions were incorporated in the NMC's first operational primitive equations limited area model, the venerable LFM (Limited-area Fine-mesh Model)."

This Eta „ancestor" code already had features that withstood the test of time: choice of the horizontal grid, and scheme for specification of the lateral boundary conditions (LBCs, Mesinger 1977). They were and are today in the Eta prescribed or extrapolated along the single outer boundary line of grid points, as it should be according to the mathematical nature of the problem.

Use of the gravity-wave coupling scheme of (Mesinger 1974) in a two-time level, split-explicit framework followed quickly thereafter, as reported in the first published note on the effort (Mesinger and Janjić 1974). Major subsequent developments include introduction of the eta coordinate (Mesinger 1984), Arakawa horizontal advection scheme on the E-grid conserving C-grid enstrophy and kinetic energy, of Janjić (1984), and the refinement of the Eta discretization making it a simple cut-cell scheme, as described in detail in Mesinger and Veljovic (2017, MV2017 later on).

It seemed appropriate to the Board on the Earth Climate System and the Opus of Milutin Milanković of the Serbian Academy of Sciences and Arts to mark the 45th anniversary of this 1973 effort with a gathering aimed in fact to looking ahead. Changes in computer architecture in progress impact the attractiveness of various model dynamical core

options. But so should the results we have. In this presentation we intend to show results which we feel should be of interest in this sense.

Eta large scale skill

While efforts of the modeling community focused on phenomena requiring increased and very high resolutions are understandable, behavior of codes for phenomena for which resolution should not be a problem deserves interest as well, and even for a special reason. This because when performance for very high resolution is not an issue, and yet major differences in code performance are identified, it makes sense to try to understand why.

With this in mind we focus on the verification of presumably larges scales of interest for weather, the tropospheric jet stream.

Driving a limited area model (LAM) by LBCs from a global model, can one improve on largest scales? MV2017 point out four requirements that need to be fulfilled by a LAM, be it in Regional Climate Modeling (RCM) or NWP environment, to improve on large scales inside its domain. First, RCM/NWP model obviously needs to be run on a relatively large domain. Note that domain size in quite inexpensive compared to resolution. Second, RCM/NWP model should not use more forcing at its lateral boundaries than required by the mathematics of the problem. That means prescribing lateral boundary conditions only at its outside boundary, with one less prognostic variable prescribed at the outflow than at the inflow parts of the boundary. Next, nudging towards the large scales of the driver model must not be used, as it would obviously be nudging in the wrong direction if the nested model can improve on large scales inside its domain. And finally, the RCM/NWP model must have features that enable development of large scales improved compared to those of the driver model. This would typically include higher resolution, but obviously does not have to.

The first convincing demonstration of an improvement in large scales by an RCM compared to those of its driver global model may have been that of Fennessy and Altshuler, presented in 2002 at an AGU meeting, and reported quite a few years later in Veljovic et al. (2010). Here we shall summarize and expand on the results of the Mesinger and Veljovic (2017, MV2017 later on) ensemble experiment in which the limited area Eta model, driven by ECMWF (EC further on) 32-day ensemble members, achieved accuracy of large scales for an extended period clearly improved compared to that of its driver members. We shall illustrate these improvements in a number of ways, aiming to enlighten as best we can how this presumably generally unexpected result could have taken place.

Needless to say, in the MV2017 Eta ensemble the first three requirements above have been fulfilled, as not doing so regarding either one of them would mean working against the objective of improving on large scales. As to the fourth one, the driven LAM required to have features enabling improved accuracy of large scales, one should note that during the first 10 days of the experiment the

resolutions of the two ensembles were about the same. Still, it was precisely during that time that a very convincing advantage of the Eta was achieved. With the resolution thus being removed from possible reasons for the Eta advantage, search for other options is obviously a matter of considerable interest.

Two verification scores were used in MV2017 to inspect the model skill in forecasting large scales: the ETS or Gilbert skill score corrected to unit bias (Mesinger 2008), and the RMS difference, for 250 hPa wind speeds > 45 m s^{-1} and compared to EC analyses. The purpose of the correction to unit bias of the ETS or Gilbert score is to have a verification of the position of the variable forecast.

Given that there is considerable evidence of the benefit the Eta model derives from its use of the eta coordinate, and in search of a test of this benefit in a larger ensemble sample, MV2017 have rerun their 21 member Eta ensemble by having the Eta switched to use sigma, Eta/sigma further on. The two scores of the driver EC ensemble, the Eta, and the Eta/sigma, are shown in Fig. 2.1.

A conspicuous feature of the scores shown is the very visible advantage of the Eta (blue) over the EC (red) during about day 2-6 of the experiment. This happens to be the time when a major upper-tropospheric trough was crossing the Rockies (MV2017, Fig. 10), a situation in which various NWP results of the operational Eta showed advantage over sigma system models ran at the time at NCEP (MV2017).

We are somewhat puzzled however by the Eta/sigma (orange) having demonstrated a visible advantage over the EC during this time as well; and in addition advantage comparable to that of the Eta later at day 7-10 time. Days 12-13 and 16-19 could be added to this list, perhaps with a bit of restraint given that at these times the skill of all models is rather low. We will show more results and add comments on possible reasons behind this Eta and also Eta/sigma skill in the following sections.

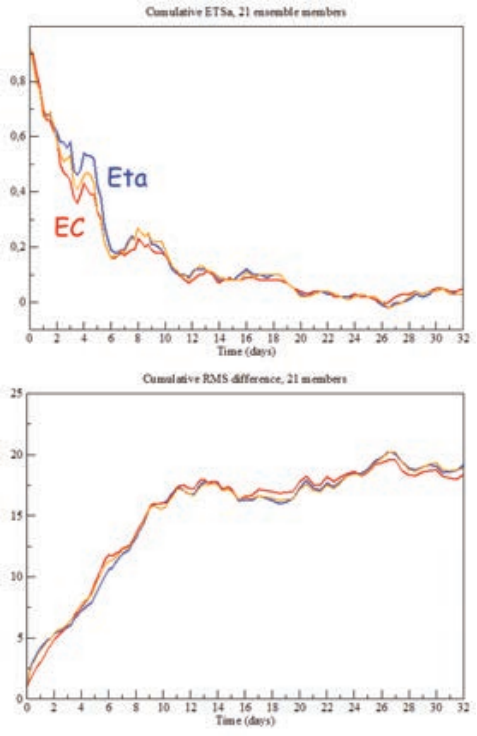

Fig. 2.1. Bias adjusted ETS (or, Gilbert) scores of wind speeds greater than 45 m s^{-1}, upper panel, and RMS wind difference, lower panel, of the driver ECMWF ensemble members (red), Eta members (blue), and Eta members run using sigma coordinate (orange), all at 250 hPa and with respect to ECMWF analyses. Initial time is 0000 UTC 4 October 2012.

Illustration: 250 hPa wind speed plots

To complement the numerical information on scores achieved, in Fig. 3.1 we show 250 hPa wind speed averages for all 21 members, at day 4.5; see figure legend for the content of its panels.

While predicting the major pattern, EC members, bottom left, do not extend the 45 m s^{-1} jet streak entering Alaska sufficiently southeastward, and have the streak across contiguous U.S. and off New England too far westward. These features are improved on Eta maps, top right, in particular by the Eta in terms of covering a bit of the eastern Labrador, and more of the ocean area off the U.S. New England states and towards the tip of Greenland.

It is interesting to note that the advantage of the Eta over Eta/sigma as seen on these average maps seems to come just about entirely from the better placement of the streak > 45 m s^{-1} over contiguous U.S. and off to northwestern Atlantic, and not from the streak entering the model domain over northern Alaska. We suspect this could be because of the flow of the former feature having had to cross the major Rocky Mountains topographic barrier, as opposed to the latter having entered the North American continent at lower elevations and east of it.

Verification via the number of "wins"

The advantage of the Eta over EC is demonstrated to even a greater degree by the number of "wins" of one model vs. another. Thus, in Fig. 4.1, left panel, number of wins of the Eta winds > 45 m s^{-1} and

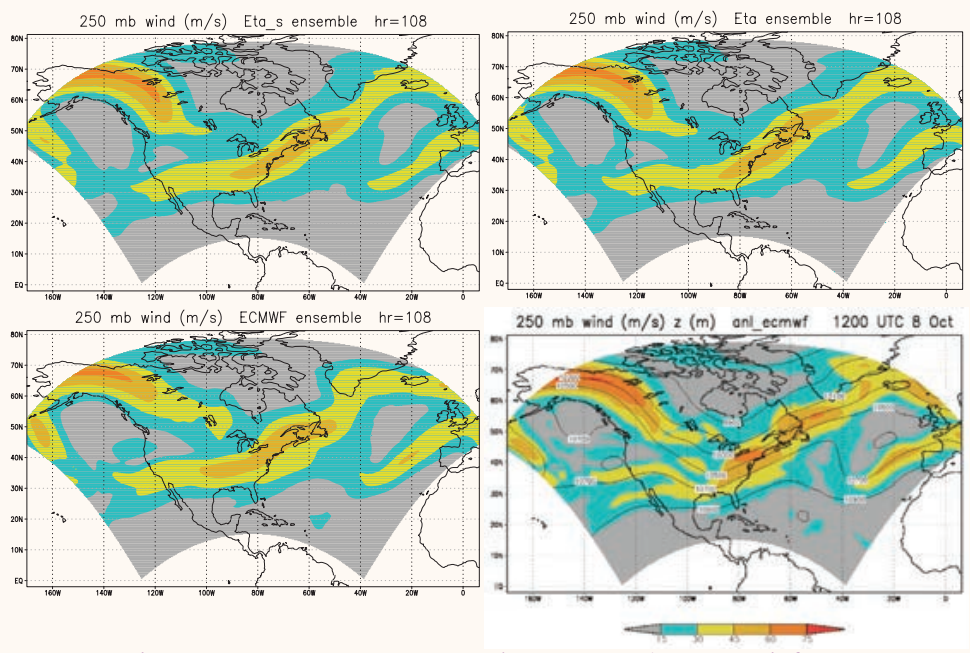

Fig. 3.1. Ensemble average, 21 members, at 4.5 day time: EC verification analysis bottom right, EC driver members bottom left, Eta members top right, Eta/sigma members top left.

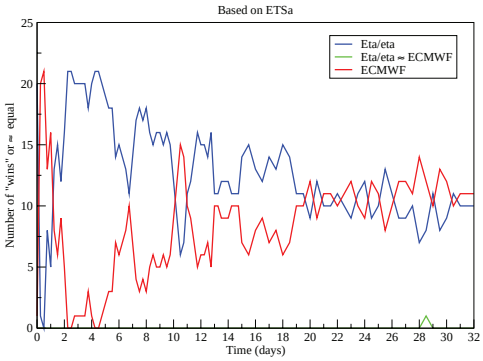

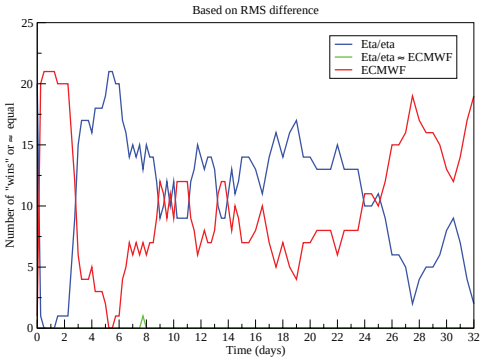

Fig. 4.1. Number of "wins" of one model vs. another: blue, Eta, red, their EC driver members. Left panel, based on ETSa scores, right panel, based on the RMS difference.

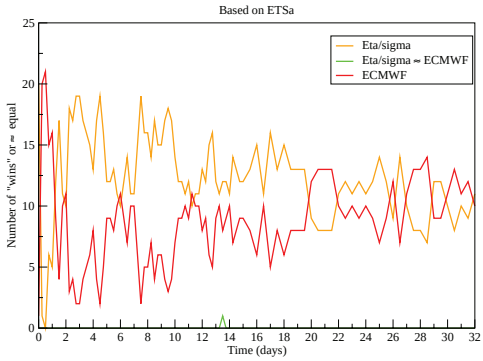

Fig. 4.2. As Fig. 4.1, left panel, but for the Eta/sigma (orange) vs. its EC driver members.

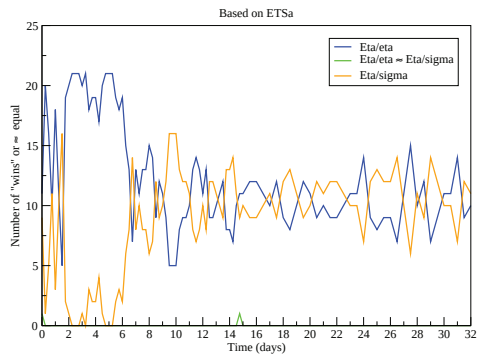

Fig. 4.3. As Fig. 4.1, left panel, but for the Eta vs. the Eta/sigma.

its EC driver members vs. each other are shown as a function of time, according to our score that verifies the accuracy of the placement of the variable verified, Equitable Threat (or Gilbert) Score adjusted to unit bias, ETSa. Same, but according to the RMS difference of forecast and analyzed winds, is shown in the right panel.

Initially the EC members are seen to have an advantage, presumably due to errors the Eta members absorb as a result of initializations off their EC driver members. The advantage of the Eta later on is particularly striking in the ETSa scores of days 2 to 6, with 4 verifications in which all 21 Eta members have better strongest winds placement scores than their EC driver members. But according to both scores the Eta members are more accurate during most of the first about 20 days or so.

An important issue is what features of the Eta are the leading contributors to its performance seen in Fig. 4.1? One feature on which we have relevant information is again the impact of the eta vs. sigma coordinate, Fig. 4.2. While the Eta/sigma is still clearly "winning" over the EC, it does not win with such a total advantage of winning repeatedly all the 21 members.

Nevertheless, reasons for the Eta/sigma performance shown being not that much inferior to that of the Eta deserve atten-

tion. In the Eta vs. Eta/sigma plot, Fig. 4.3, overwhelming advantage of the Eta is however seen in the early period, with 7 wins for all the 21 Eta members during the early time of the upper tropospheric trough crossing the Rockies.

Features possibly helping the Eta/sigma display such a perhaps unexpected advantage over the EC as seen in Fig. 4.2 are discussed at some length in our MV2017 reference. Briefly, we feel among the leading candidates are our Arakawa horizontal advection scheme (Janjić 1984), finite-volume van Leer type vertical advection of all variables (Mesinger and Jovic 2002), and perhaps also very careful construction of model topography (MY2017), with grid cell values selected between their mean and silhouette values, depending on surrounding values, and no smoothing. Exact conservation of energy in space differencing in transformation between the kinetic and potential energy is yet another candidate, as we are not aware of this conservation being enforced in other production NWP models.

More verification results

Given that our score that we emphasized the most, ETSa, is not widely used, we made an effort to verify our results with yet another measure of skill, Extreme Dependency Score (EDS), designed specifically for forecasts of rare events (Stephenson et al. 2008). EDS addresses the problem of many scores of having a non-informative limit for increasing rarity of events, and does not explicitly depend on the bias of the forecasting system.

In Fig. 5 we show the number of "wins" of the Eta model in two versions vs. the EC, according to the EDS. The Eta, left panel, blue, achieves even greater dominance over the EC than it does according to the ETSa, now with as many as 11 verifications in which all 21 Eta members had better EDS scores than their EC driver members. The Eta switched to sigma, right panel, orange, also does well, but achieves only 3 verifications in which all of its members had better score than their drivers. That however is still greater advantage over the EC than according to the ETSa score, Fig. 4.2.

We end these additional verifications with one more graphical illustration, that of the contours of areas of 250 hPa wind speeds > 45 m s^{-1}, achieved by the three models. In Fig. 5.2, upper panel, in yellow-brown we show contours of the

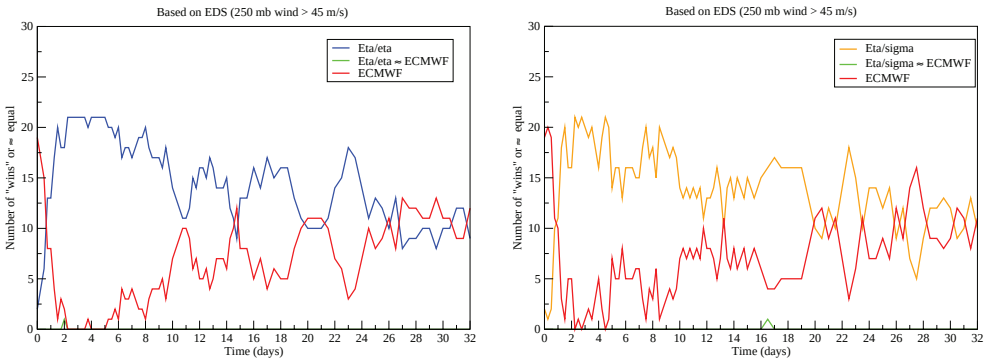

Fig. 5.1. Left: as in the left panel of Fig. 4.1, but according to the EDS; right: as in Fig. 4.2, but according to the EDS.

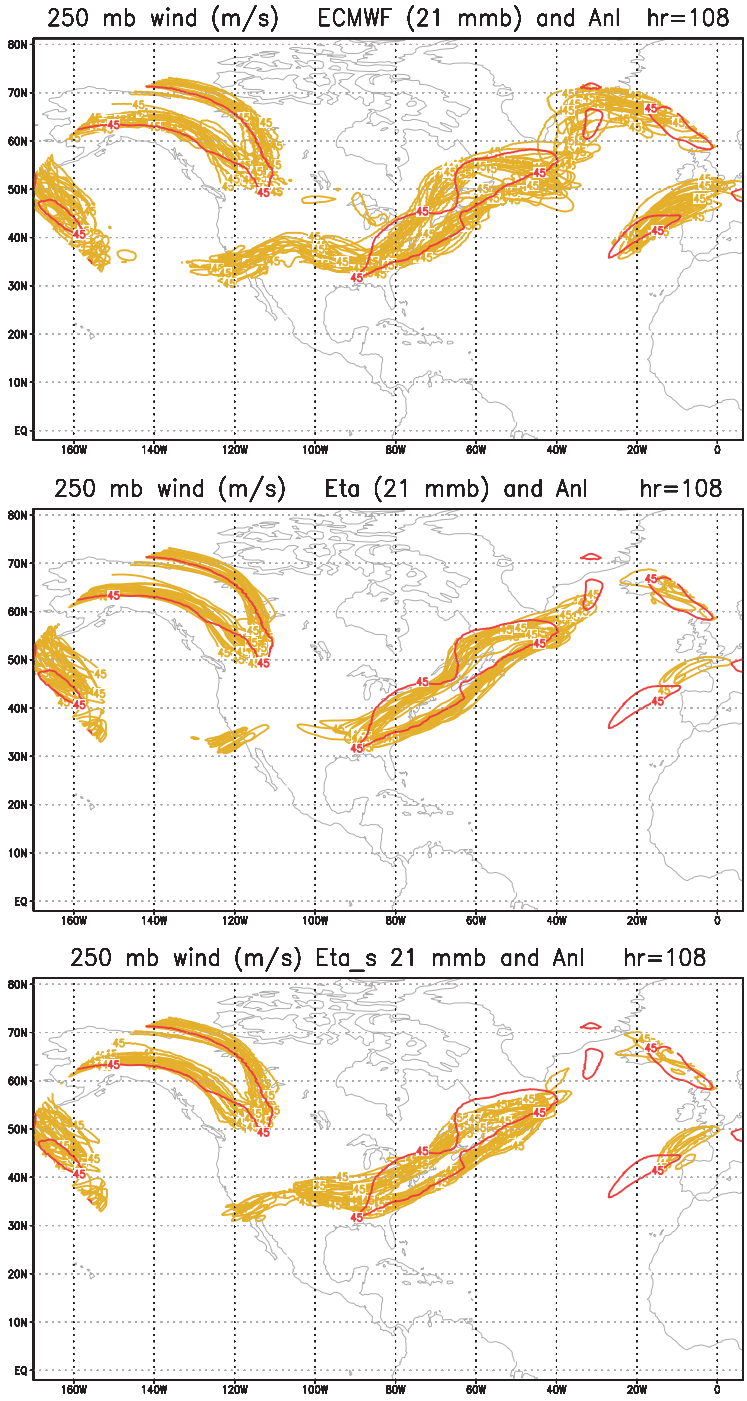

Fig. 5.2. Contours of the areas of 250 hPa wind speeds > 45 m s-1 of 21 members of the EC driver ensemble, upper panel, the Eta ensemble, middle panel, and the Eta/sigma ensemble, lower panel, all yellow-brown, and of the EC verification analysis, red; at 4.5 day lead time.

250 hPa wind speeds > 45 m s^{-1} of the 21 EC driver members at 4.5 day lead time, along with verification contours, in red. We chose the 4.5 day lead time because it is the longest of the 4 verification times with all 21 Eta members winning the ETSa scores against their EC drivers. In the middle panel we show the same, except for the 21 Eta members; and in the lower panel the same, but for the Eta/sigma members.

Referring if we may to the areas of speeds greater than 45 m s^{-1} as jet stream, while the contours of various jet streaks generated by the EC members, upper panel, are generally in the right places, tendencies to include some areas which did not verify are present as well. In particular, numerous contours erroneously extend across central and southern U.S. all the way into the eastern Pacific. Another area of unsatisfactory coverage is over southeastern Greenland and east of it, once again over a region mostly in the lee of high topography. One more feature that did not verify is the coverage by perhaps all EC contours of considerable part of the Labrador peninsula.

All of these weaknesses are almost completely absent in the Eta ensemble contours, middle panel. Forecast contours corresponding to the analyzed position and even shape of the jet streak extending from the eastern U.S. across northeastern Atlantic display no member with a very large departure from the analysis. Contours of the Eta/sigma ensemble, bottom panel, are also much improved compared to the EC contours, but do contain many members extending across the central U.S., some of them all the way to the eastern Pacific.

Concluding remarks

We are in this extended abstract making two key points. First, our experiment we feel demonstrates that running a limited area model such as an RCM, driven by a global model, improvement of large scales of the driver model is possible. This fact invalidates justifications of two widespread paradigms of RCM modeling: of using Davies' relaxation LBC scheme, and of performing large-scale or spectral nudging inside the RCM domain.

Having obtained the improvements shown by running our limited area Eta model without resorting to resolution higher than that of the driver EC model, our second key point is that the Eta model's dynamical core just about has to contain features responsible for the improvements achieved. Note by the way words of the recent review of numerical methods by Côté et al. (2015), that "Although spectral transform methods are being predicted to be phased out, the current spectral model at the European Centre for Medium-Range Weather Forecasts… is the benchmark to beat, and it is not clear that any of the new developments are ready to replace it."

Of the Eta features that to this end deserve attention, the quasi-horizontal coordinate surfaces of the Eta and its cut-cell approach we believe have here been convincingly demonstrated as a priority. Note that experiments of Steppeler et al. (2013) using a different cut-cell approach just as well strongly suggest that abandoning the terrain-following coordinates in favor of coordinates intersecting topography should help increase the skill of atmospheric weather and climate models.

But clearly some of the other Eta dynamical core features, as suggested at the end of our Section 4, are very much worth exploring.

References

Côté J, Jablonowski C, Bauer P, Wedi N (2015) Numerical methods of the atmosphere and ocean. Seamless prediction of the Earth system: From minutes to months, 101–124. World Meteorological Organization, WMO-No. 1156.

Janjić ZI (1984) Nonlinear advection schemes and energy cascade on semi-staggered grids. Mon. Weather Rev. 112, 1234–1245. doi:10.1175/1520-0493(1984)112<1234:NASAEC>2.0.CO;2

Mesinger F (1974) An economical explicit scheme which inherently prevents the false two-grid-interval wave in the forecast fields. Proc. Symp. "Difference and Spectral Methods for Atmosphere and Ocean Dynamics Problems", Academy of Sciences, Novosibirsk 1973; Part II, 18-34

Mesinger F (1977) Forward-backward scheme, and its use in a limited area model. Contrib. Atmos. Phys., 50, 200-210.

Mesinger F (1984) A blocking technique for representation of mountains in atmospheric models. Riv. Meteor. Aeronautica, 44, 195-202

Mesinger F (2004) The Eta Model: Design, history, performance, what lessons have we learned? Symp. on the 50th Anniversary of Operational Numerical Weather Prediction, Univ. of Maryland, College Park, MD, 14-17 June 2004, 20 pp. http://www.ncep.noaa.gov/nwp50/Agenda/Tuesday/

Mesinger F (2008) Bias adjusted precipitation threat scores. Adv. Geosci., 16, 137–143. doi:10.5194/adgeo-16-137-2008

Mesinger F, Janjic ZI (1974) Noise due to time-dependent boundary conditions in limited area models. The GARP Programme on Numerical Experimentation, Rep. 4, WMO, Geneva, 31-32.

Mesinger F, Jovic D (2002) The Eta slope adjustment: contender for an optimal steepening in a piecewise-linear advection scheme? Comparison tests. NCEP Office Note 439. http://www.emc.ncep.noaa.gov/officenotes/index.shtml

Mesinger F, Veljovic K (2017) Eta vs. sigma: Review of past results, Gallus-Klemp test, and large-scale wind skill in ensemble experiments. Meteorol. Atmos. Phys., 129, 573-593. doi:10.1007/s00703-016-0496-3

NWS (1973) Numerical Weather Prediction Activities: National Meteorological Center, First Half 1973. U.S. Dept. of Commerce, NOAA, National Weather Service, Silver Spring, MD, 36 pp.

Steppeler J, Park S-H, Dobler A (2013) Forecasts covering one month using a cut-cell model. Geosci. Model Dev., 6, 875-882. doi:10.5194/gmd-6-875-2013

Veljovic K, Rajkovic B, Fennessy MJ, Altshuler EL, Mesinger F (2010) Regional climate modeling: Should one attempt improving on the large scales? Lateral boundary condition scheme: any impact? Meteor. Zeitschrift, 19, 237–246. doi:10.1127/0941-2948/2010/0460

Numerical Modeling of the Atmosphere: A Review

Miodrag Rančić[1] and Fedor Mesinger[2]

[1] IMSG at NCEP/NOAA, College Park, Maryland, USA (miodrag.rancic@noaa.gov)

[2] Serbian Academy of Sciences and Arts, Belgrade, Serbia (fedor.mesinger@gmail.com)

Introduction

This paper intents to summarize some of the most important elements of methods used in formulation of numerical models of atmospheric dynamics. The organization of the presentation closely follows a recent more comprehensive review paper by Mesinger et al. (2018), but here we try to deliver more attention to the latest, most promising developments. More deatiled reviews of the subject can be found in textbooks, such as Kalnay (2003) and Durran (2010), and the review articles, such as Cullen (2007), Lauritzen et al. (2011) and Côté et al. (2015).

Underlining principles and related issues

Bjerknes (1904) was the first one who pointed out that given the initial field of state variables, and knowing equations that govern their evolution in time, one should be able to find their future state.

However, a series of issues had to be understood and resolved in order to produce first realistic weather forecasts.

One of the issues is that we do not exactly know atmospheric fields except at certain points in space and time. Our continuous equations that express physical laws that govern behavior of the atmosphere, even if we were able to solve them analytically in the general case (which we do not!) are not applicable for the case with such a limited knowledge ("finite degrees of freedom"), and we need to use their approximations and solve them using approximate methods. In doing so, we need to use the "representative" rather than "instantaneous values" of the variables, which could lead to misleading results. For example, the famous first numerical forecast attempt by Richardson (1922) was in a later reconstruction (e.g., Lynch 1999) surprisingly successful only by including spatial filtering of the initial fields.

Secondly, equations of the atmospheric dynamics have a series of physical constraints ("mimetic properties") that a realistic solution of approximate equations needs to reflect. That includes: conservation of mass, energy, rotational properties and positiveness of the solution in the case of atmospheric tracers, which are not automatically nor easy reproduced with the approximate solutions.

On top of that, atmospheric equations are nonlinear, and in addition also cha-

Fig. 2.1. From left to right: Vilhelm Bjerknes, Lewis Fry Richardson, Norman Phillips, Edward Lorenz, and Akio Arakawa.

otic, making our task all but hopeless. Namely, as pointed out by Lorenz (1960), small perturbations in the initial conditions can lead to qualitatively different solutions.

Solving the systems of algebraic equations that approximate continuous atmospheric equations introduces new issues, such as numerical instabilities. In order to prevent a linear instability, a limitation on time-step for propagating solution in time has to be imposed, known as a Courant-Friedrichs-Lewy condition.

Phillips (1956) discovered a different, nonlinear computational instability, which he later explained in his (1959) paper as an erroneous accumulation of energy at the shortest scales. That led Arakawa (1966) to devise an advection scheme which, by conserving chosen integral properties of the continuous equations, eliminated the problem and became a forerunner of later efforts in emulating various properties of the physical system.

Typically, numerical techniques used for solving the approximate systems of equations generate computational noise and suffer from an inadequate numerical dispersion of the short waves which are not well represented in numerical simulations. At the same time, the impact from the physics forcing generally takes part precisely in the short part of the spectrum, where our skill is minimal, and the short waves are those responsible for spreading the influence of this forcing into surrounding.

In addition, energy dissipation takes place in the real atmosphere at scales still far beyond our practical rich ("subgrid scales"), and the models use different mechanisms to describe this subscale dissipation, such as horizontal diffusion, divergence damping, smoothers, filters and fixers, as neatly described in a review of the subject provided in Jablonowski and Williamson (2011).

There is no universal theory how to deal with this issue, though a limited guidance come from Smagorinsky (1993). One objective criterium of how successfully model deal with the subgrid dissipation was suggested by Skamarock (2004, 2011), who introduced a model's "effective resolution" as the one at which kinetic energy spectrum (KE) starts to be steeper then k^(-5/3) observed in atmosphere for higher wave numbers. For models that ever came close to following this law, that is between 6 and 10 grid intervals.

In spite of all these difficulties, construction of the Electronic Numerical Integrator and Computer (ENIAC), the first

general-purpose electronic digital computer, in 1943–1945, enabled Charney et al. (1950) to produce a pioneering weather forecast by a numerical integration of the barotropic vorticity equation which opened the door for a dynamical development of this field.

Various approaches to numerical modeling

Among many techniques used for numerical modeling of the atmosphere, a distinguished place belongs to finite-differencing techniques, that were prevailingly used for regional models during twentieth century, and spectral techniques, that were used for global models. In terms of where is located the updated variables, they both belong to a group of Eulerian methods. On the other end are Lagrangian methods, where the variables are updated following motion of the air. In the modeling of atmosphere more common are semi-Lagrangian methods, where values in the Lagrangian particles are occasionally remapped back to the grid points fixed in space. A mass conservative version of semi-Lagrangian method is illustrated in Fig. 3.1.

In recent years, it appears that the finite-volume and spectral element methods are taking the lead. Generally, with the revolutionary advent of massively parallel computers, and expectations that numerical models will be in near future run on order of tens of thousands of processors, numerical techniques based on application of global operators, such as spectral methods, gradually but steadily lose the ground and are being replaced with the sophisticated technics based on application of local operators,

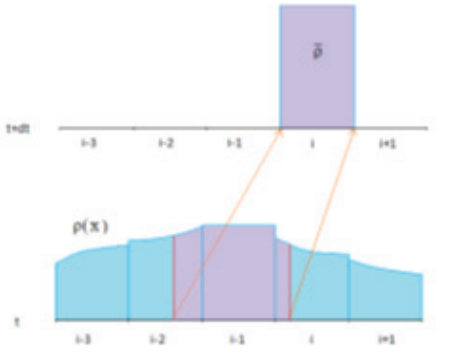

Fig. 3.1. Given average densities ($\bar{\rho}$) over grid boxes at the initial time level are updated by: (1) first assuming a piecewise distribution of density across domain, ρ(x), (2) then by casting backward trajectories from time level t + dt to level t, and (3) finally by calculating mass between departure points that will arrive into a box i at the next time level, comprising the new average density in the arrival grid box. (Rančić, 1992).

such as finite-volume methods, which minimize communication between processing elements.

The presentation will briefly summarize the major features of all these techniques.

Representation of spherical Earth

With the prospect of abandoning spectral methods in global models of the atmosphere, and because of the problems that convergence of meridians toward poles on the standard spherical grid introduces to local methods, the new quasi-uniform topologies for casting grid points over the globe become subject of intensive research. A comprehensive review of the subject is found in Staniforth and Tuburn (2012).

The grids derived by projection of various polyhedrons to the sphere (such as

"cubed-spheres" shown in Fig. 4.1) provide a continuous gridding of the sphere, making relatively easy to satisfy the mimetic constraints. However, these grids are generally made by the curvilinear coordinates, which requires a transformation of the governing equations and creates new issues, such as, for example, grid-imprints (e.g., Piexoto and Barros, 2013). Still, the US Weather Service recently adopted FV3, a finite-volume model operating on a cubed sphere, developed by S.-J. Lin and collaborators at GFDL, as the main forecasting instrument.

An alternative approach is a technique of overlapping (or oversetting) grids, which avoids the need for curvilinear formulation, but requires a special treatment in the overlap regions and generally does not automatically satisfy conservation constraints.

The unstructured grids started attracting attention lately because of their grid adapting capability. For example, ECMWF is developing an unstructured grid component (Smolarkiewicz et al. 2015). We show on Fig. 4.3 a semi-unstructured Fibonacci grid that combines a natural coordinate smoothness with many properties of fully unstructured grids.

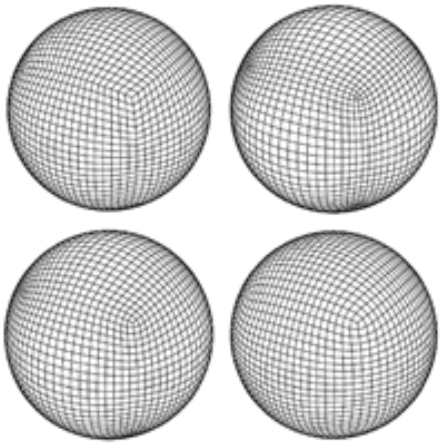

Fig. 4.1. Various cubed-spheres. Upper left, gnomonic (Sadourny, 1972); upper right, conformal (Rančić et al., 1996); lower left, smoothed conformal (Purser & Rančić, 1998); lower right, uniform-Jacobian (Rančić et al., 2017).

Nonhydrostatic models

As a rule, various approximations were used in practice in order to simplify and speed up operation of numerical models, such as, hydrostatic, traditional, the approximation of the shallow-atmosphere, Boussinesq, anelastic, and various quasi incompressible approximations. The relative shallowness of the troposphere (between 7 km in the polar regions and 20 km in the tropics), made especially

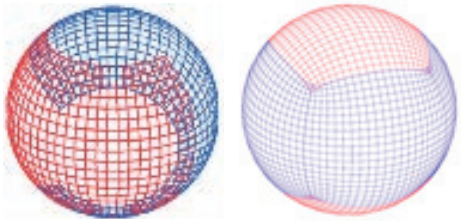

Fig. 4.2. Examples of overlapping grids. On left Yin-Yang grid (from Staniforth and Thuburn, 2012); on right, overlapped conformal cubed-sphere (from Purser 2017).

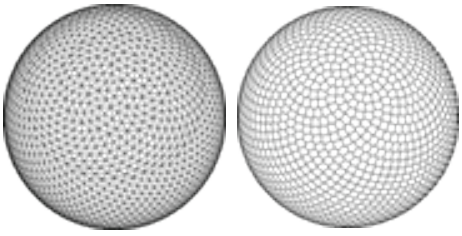

Fig. 4.3. Fibonacci grid. On left: Delaunay triangulation (showing nodes); on right: Voronoi mesh (showing cells). (From Swinbank and Purser, 2006).

the hydrostatic approximation, which replaces the component of the equation of motion in the vertical with the hydrostatic balance condition, a common feature of the prognostic and climate models of the atmosphere for many years. This approximation filters out vertically propagating fast sound waves, making computation much more efficient. However, at the beginning of the 21st century, full compressible, nonhydrostatic models become standard. In the recent U.S. Next Generation Global Prediction System (NGGPS) competition, every participating group presented a fully compressibe, nonhydrostatic model: the Nonhydrostatic Icosahedral Model (NIM) from the NOAA/ESRL (Bleck et al., 2015); the Model for Prediction Across Scales (MPAS) from NCAR (Skamarock et al., 2012); NEPTUNE from the U.S. Naval Research Laboratory (NRL), using the dynamical core of the Nonhydrostatic Unified Model of the Atmosphere, NUMA (e.g., Giraldo, et al. 2013); FV3 from NOAA/GFDL (e. g., Harris and Lin, 2013); and the uniform-Jacobian (UJ) version of the Nonhydrostatic Multiscale Model (NMM-UJ) from NOAA/NCEP (Rančić, et al. 2017).

Emerging methods

At this point in time, it looks that future belongs to the *finite-volume* and, maybe in the later stage, *discontinuous Galerkin* (DG) (a subgroup of spectral element) methods.

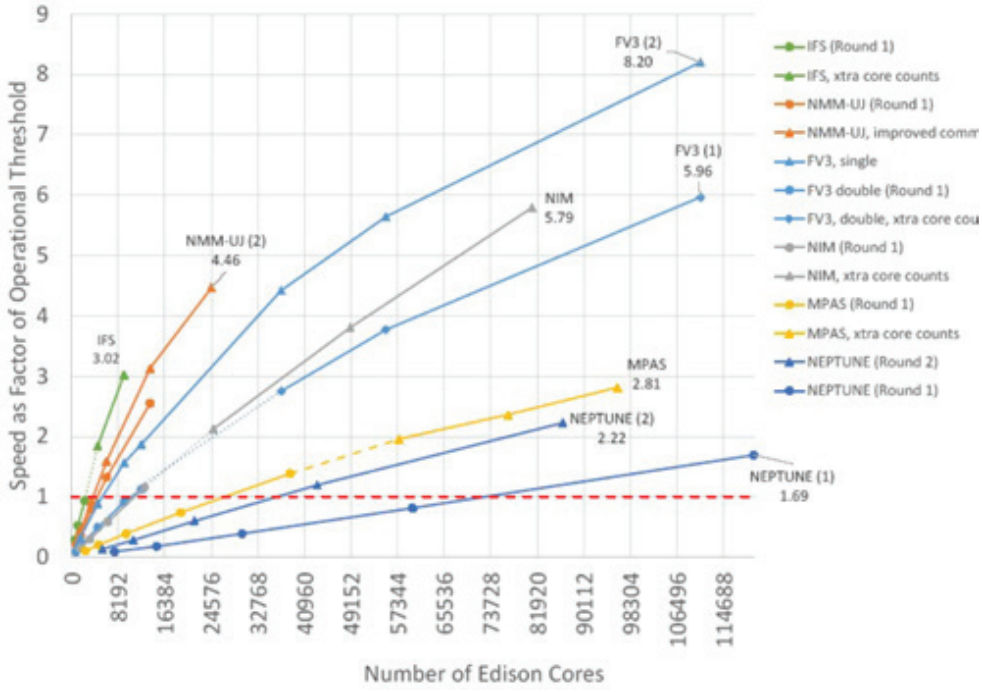

Fig. 5.1. Scalability of the suite of global models in a 3-km run according to the NGGPS report. The plot shows speed up for 3-min simulation using a log-log scale. Higher is better. The model of ECMWF (IFS) was run with the hydrostatic approximation. From Michalakes et al. (2015).

Finite-volume methods easily adjust to quasi-uniform and unstructured grids; they can satisfy most important mimetic constraints; and use only local operators, which is good for parallelization. However, they generally have a low (usually 3rd) order of accuracy, which is believed to be to some extent compensated by the high resolutions available to contemporary computers. Both model finalists in the mentioned NGGPS competition (FV3 and MPAS) are finite volume models. Perhaps the best introduction into finite-volume methods is found in LeVeque (2002).

Unlike finite-difference methods, which deal with the grid-point (nodal) values, finite-volume methods operate with the grid-box averaged values. Let us consider a mass conservation equation:

$$\frac{\partial \rho}{\partial t} + \nabla \cdot (\rho \mathbf{V}) = 0 \quad \Big/ \int_S dS$$

which we would like to solve on an arbitrary unstructured grid shown in Fig. 6.1. We first take an integral over area S of a grid-box, which results in

$$\frac{\partial \overline{\rho}}{\partial t} + \int_S \nabla \cdot (\rho \mathbf{V}) dS = 0$$

Here $\overline{\rho}$ is the grid-box averaged value (mass) whose evolution in time we would like to calculate. By applying Gauss theorem, we can convert surface integral into a line integral along boundary of the grid-box:

$$\frac{\partial \overline{\rho}}{\partial t} + \oint_L (\rho \mathbf{V}) \cdot \mathbf{n} dl = 0$$

The terms within brackets now represent fluxes (F) through the boundary of the grid box, and the final solution, after taking an integral in time, can be expressed as

$$\overline{\rho}(t + \Delta t) = \overline{\rho}(t) - \int_t^{t+\Delta t} \left(\oint_L \mathbf{F} \cdot \mathbf{n} dl \right) dt$$

Practically, the time change of the average value of a variable in the grid-box is result of time integral of its fluxes across boundaries (Godunov, 1959). The estimation of the time integral of fluxes is referred to as Riemann solver. It could be solved exactly in 1D case, but only approximately in the 2D case.

Fig. 6.1. Arbitrary unstructured grid on the left. A schematic illustration of the finite-volume numerical procedure on the right.

DG method, which was introduced in Reed and Hill (1973) and Cockburn et al. (2002), has a higher-order of accuracy, and is inherently conservative. An excellent review of this method is provided by Nair et al. (2011). In modeling of the atmosphere, forerunners of DG method are Nair (2009) and Giraldo et al. (2013). In comparison with the finite-volume method, DG carries more information per a control volume evolving in time, and could be thought of as a high-order (or even "spectral") version of the finite-volume method.

Another very interesting development represent exponential time integration methods, which recently found their way into meteorological literature (e.g., Gaudreault and Pudykiewicz, 2016). These techniques promise to accurate-

ly describe high frequencies, and still use time steps larger than semi-implicit methods.

A major development in the modeling of vertical structure of the atmosphere presents a vertically-Lagrangian coordinate (e.g., Chen et al. 2013). The "shaved" (or, cut-cell, sloped) representation of terrain (e.g., Mesinger and Jovic, 2002; Steppeler et al. 2013; Shaw and Weller 2016) is also getting in the focus of many research groups.

Though contra intuitive, there is an abundance of literature describing methods for parallelization in time. A review of this subject can be found in Gander and Hairer (2015). One reason to consider these methods is an assumption that the number of available processors will increase faster than the resolution of the models. In applications in meteorology a practical version of this method will probably consist of a series of predictor (parallel) and corrector (sequential) trials. An early application of these methods in meteorology was done by Côté (2012).

References

Arakawa A (1966) Computational design for long-term numerical integration of equations of fluid motion: Two-dimensional incompressible flow. Part I. J. Comp. Phys., **1,** 119–143. (Reprinted in J. Comp. Phys., **135,** 103–114.)

Bjerknes V (1904) Das Problem der Wettervorhersage, betrachtet vom Standpunkte der Mechanik und der Physik. Met. Zeit., **21**, 1-7. (Translation by Y. Mintz: The problem of weather forecasting as a problem in mechanics and physics. Los Angeles, 1954. Reprinted (pp 1-4) in Shapiro and Grønås, 1999.)

Bleck R, Bao J, Benjamin S, Brown J, Fiorino M, Henderson T, Lee J, MacDonald A, Madden P, Middlecoff J, Rosinski J, Smirnova T, Sun S, Wang N (2015) A vertically flow-following icosahedral grid model for medium-range and seasonal prediction. Part 1: Model description. Mon. Wea. Rev., **143,** 2386–2403.

Charney JG, Fjørtoft R, von Neumann J (1950) Numerical integration of the barotropic vorticity equation. Tellus, **2,** 237–254.

Cockburn B, Karniadakis GE, Shu CW (2000) The development of discontinuous Galerkin methods. In Discontinuous Galerkin Methods: Theory, Computation, and Applications. Lecture Notes in Computational Science and Engineering. **11**, Springer, 470 pp.

Côté J (2012) Time-parallel algorithms for weather prediction and climate simulation. Seminar at Isaac Newton Institute for Mathematical Sciences, Oct. 23, 2012.

Côté J, Jablonowski C, Bauer P, Wedi N (2015) Numerical methods of the atmosphere and ocean. In *Seamless prediction of the Earth system: From minutes to months*. World Meteorol. Org., WMO-No. 1156, 101-124.

Cullen MJP (2007) Modelling atmospheric flows. Acta Numerica, Cambridge Univ. Press, 1-87.

Durran DR (2010) Numerical Methods for Fluid Dynamics, with Applications to Geophysics. Series: Texts in Applied Mathematics, **32**, 2nd Edition., 2010, XV, 516 pp.

Gander MJ, Hairer E (2008) Nonlinear convergence analysis for the parallel algorithm. In *Domain Decomposition Methods in Science and Engineering* XVII, O. B. Widlund and D. E. Keyes, eds., Lecture Notes in Computational Science and Engineering, Springer, 60:45–56.

Gaudreault S, Pudykiewicz JA (2016) An efficient exponential time integration method for the numerical solution of the shallow water equations on the sphere. J. Comp. Phys., **322,** 827–848.

Giraldo FX, Kelly JF, Constantinescu EM (2013) Implicit-explicit formulations of a three-dimensional nonhydrostatic unified model of the atmosphere (NUMA). SIAM Journal on Scientific Computing, **35,** B1162–B1194.

Godunov SK (1959) A difference method for numerical calculation of discontinuous solutions of the equations of hydrodynamics. Mat. Sb. (N.S.), 47(**89**), 271–306.

Harris LM, Lin S-J (2013) A two-way nested global-regional dynamical core on the cubed-sphere grid. Mon. Wea. Rev., **141,** 283–306.

Jablonowski C, Williamson DL (2011) The pros and cons of diffusion, filters and fixers in atmospheric general circulation models. In P. H. Lauritzen et al., (Eds.), *Numerical Techniques for Global Atmospheric Models*, LNCSE **80,** Springer-Verlag, 381-493.

Kalnay E (2003) *Atmospheric Modeling, Data Assimilation and Predictability*. Cambr. Univ. Press, 320 pp.

Lauritzen PH, Jablonowski C, Taylor MA, Nair RD, Eds. (2011) *Numerical Techniques for Global Atmospheric Models*, Lecture Notes in Computational Science and Engineering, Springer, **80**, 556 pp.

LeVeque RJ (2002) *Finite Volume Methods for Hyperbolic Problems*. Cambridge Texts in Applied Mathematics. Cambr. Univ. Press, 558 pp.

Lorenz EN (1960) Energy and numerical weather prediction. Tellus, **12,** 364–373.

Lynch P (1999) Richardson's marvelous forecast. In "The Life Cycles of Extratropical Cyclones", ed. M. A. Shapiro and S. Grønås. Boston: Am. Met. Soc, 61-73.

Mesinger F, Rančić M, Purser RJ (2018) Numerical Methods in Numerical Models. *Oxford Research Encyclopedia of Climate Science,* (in press).

Mesinger F, Jovic D (2002) The Eta slope adjustment: Contender for an optimal steepening in a piecewise-linear advection scheme? Comparison tests. NOAA/NCEP Office Note 439, 29 pp.

Michalakes J, Coauthors (2015) *Advanced Computing Evaluation Committee Report: NGGPS Level-1 Benchmarks and Software Evaluation*. 22 pp. http://www.nws.noaa

Nair RD (2009) Diffusion experiments with a global discontinuous Galerkin shallow-water model. Mon. Wea. Rev., **137,** 3339–3350.

Nair RD, Levy MN, Lauritzen PH (2011). Emerging numerical methods for atmospheric modeling. In P. H. Lauritzen et al., (Eds.), *Numerical Techniques for Global Atmospheric Models*, LNCSE **80**, Springer-Verlag, 189-250.

Phillips NA (1956) The general circulation of the atmosphere: A numerical

experiment. Quart. J. Roy. Met. Soc., **82,** 123–164.

Phillips NA (1959) An example of non-linear computational instability. In: *The Atmosphere and the Sea in Motion.* New York, Rockefeller Institute Press, 501-504.

Peixoto PS, Barros RM (2013) Analysis of grid imprinting on geodesic spherical icosahedral grids. J. Comp. Phys., **23,** 61–78.

Purser RJ (2017) Conformal localized overset polyhedral global grids based on Riemann surfaces. WGNE Blue Book, 2017, 3-05–3-06.

Purser RJ, Rančić M (1998) Smooth quasi-homogenous gridding of the sphere. Quart. J. Roy. Met. Soc., **124,** 637–647.

Rančić M (1992) Semi-Lagrangian piecewise biparabolic scheme for two-dimensional horizontal advection of a passive scalar. Mon. Wea. Rev., **120,** 1394-1406.

Rančić M, Purser RJ, Mesinger F (1996) A global shallow-water model using an expanded spherical cube: Gnomonic versus conformal coordinates. Quart. J. Roy. Met. Soc., **122,** 959–982.

Rančić M, Purser RJ, Jović D, Vasic R, Black T (2017) A nonhydrostatic multiscale model on the uniform Jacobian cubed-sphere. Mon. Wea. Rev., **145,** 1083-1105.

Richardson LF (1926) Atmospheric diffusion shown on a distance-neighbor graph. *Proceedings of the Royal Society of London. Series A,* **110**: 709–737.

Reed WH, Hill TR (1973) Triangular mesh method for neutron transport equation. In *Technical Report. LA-UR-73-479,* Los Alamos Scientific Laboratory.

Sadourny R (1972) Conservative finite-differencing approximations of the primitive equations on quasi-uniform spherical grids. Mon. Wea. Rev., **100,** 136–144.

Shaw J, Weller H (2016) Comparison of terrain-following and cut-cell grids using a nonhydrostatic model. Mon. Wea. Rev., **144,** 2085-2099.

Skamarock WC (2004) Evaluating mesoscale NWP models using kinetic energy spectra. Mon. Wea. Rev., **132,** 3019–3032.

Skamarock WC (2011) Kinetic energy spectra and model filters. In P. H. Lauritzen et al., (Eds.), *Numerical Techniques for Global Atmospheric Models*, LNCSE **80**, Springer-Verlag. 495–512.

Skamarock WC, Klemp JB, Duda MG, Fowler LD, Park, S-H, Ringler TD (2012) A multiscale nonhydrostatic atmospheric model using centroidal Voronoi tessellations and C-grid staggering. Mon. Wea. Rev., **140,** 3090–3105.

Smagorinsky J (1993) Some historical remarks on the use of nonlinear viscosities. In B. Galperin & S. A. Orszag (Eds.) *Large Eddy Simulation of Complex Engineering and Geophysical Flows,* Cambr. Univ. Press, 3-36.

Smolarkiewicz P, Deconinck W, Hamrud M, Kühnlein C, Mozdzynski G, Szmelter J, Wedi N (2015) An all-scale, finite volume module for the IFS. ECMWF Newsletter No. 145, 24–29.

Staniforth A, Thuburn J (2012) Horizontal grids for global weather and

climate prediction models: a review. Quart. J. Roy. Met. Soc., **138,** 1–26.

Steppeler J, Park S-H, Dobler A (2013) Forecasts covering one month using a cut-cell model. Geoscientific Model Development, **6,** 875–882.

Swinbank R, Purser RJ (2006) Fibonacci grid: A novel approach to numerical modeling. Quart. J. Roy. Met. Soc., **132,** 1769–1793.

Cloud parameterization and cloud prediction scheme in the Eta numerical weather model

Ivan Ristic[1], *Ivana Kordic*[2]

[1] Weather2, Belgrade, Serbia (ivanr@weather2.rs)
[2] Weather2, Belgrade, Serbia (ivana.kordic@weather2.rs)

Abstract

To improve cloud and precipitation forecast we developed new cloud prediction scheme and we implemented it in Eta model. Fractional cloud cover, cloud liquid water, cloud ice and cloud snow are explicitly predicted by adding three prognostic equations for fractional cloud cover, cloud mixing ratio and snow per cloud fraction to the model. Sedimentation of ice and snow is also included in parameterization. Precipitation of rain and snow are determined from cloud fields. Clouds predicted like this can be used also in radiation parameterization.

Thermodynamic wet bulb temperature will be used for describing clouds because it is constant during water phase changes. By using this temperature moist static energy of model grid box and cloudy part inside the grid box is the same and principle of energy conservation is satisfied.

Integration of the model for test cases indicate that new cloud prediction scheme improved forecast compared to the original model. New fractional cloud cover formula showed good results in practice, since the fractional cloud cover, predicted in this way, was much closer to the real cloud cover values. Significant progress has been made in stratiform precipitation forecast. Positive impact on convection scheme is also noticed. Validation of these test cases will be presented in this paper.

The CMCC Operational Seasonal Prediction Modelling System

Stefano Tibaldi[1], Antonella Sanna[1], Andrea Borrelli[1], Davide Padeletti[1], Silvio Gualdi[1] and Antonio Navarra[1]

[1] CMCC - Centro Euro-Mediterraneo sui Cambiamenti Climatici, Via C. Berti Pichat 6/2, 40127 Bologna, Italy (stefano.tibaldi@cmcc.it)

Introduction

The presentation will describe the new Seasonal Prediction System developed at CMCC to perform seasonal forecasts operationally (CMCC-SPS3). The system is used to provide monthly ensemble (50 members) operational seasonal predictions up to six months for the Copernicus Climate Data Store, under contract from ECMWF, together with similar operational forecasts from UKMO, Meteo France, DWD and ECMWF itself.

The CMCC Seasonal Prediction System

A more realistic representation of the Climate System components such as the ocean, the sea ice, the snow cover, the soil moisture and the stratosphere is crucial to obtain reliable forecasts at the sub-seasonal to seasonal time-scale. The Seasonal Prediction System currently operational at the Euro-Mediterranean Center on Climate Change (CMCC-SPS3) was indeed developed with the aim of achieving enhanced predictive skill in a variety of different aspects. In comparison to the previous system (SPS2), the new model has a completely different dynamical core, based on the new CMCC Earth System Model (Fogli and Iovino, 2014). The new system features a better horizontal resolution of both the atmospheric and oceanic components, better representation of the stratosphere, more realistic initialization procedures for atmosphere, land, sea and ice modules and a larger operational ensemble size (50 members). Such improvements have a positive impact on the model climate and on the predictive skill of the new system.

Fig, 2.1. Scheme of the CMCC-SPS3 fully coupled Seasonal Prediction System.

The Operational CMCC Seasonal Prediction System is based on a number of global forecast modules interlinked by a coupler/driver taking care of the communication tasks between such modules (see Figure 2.1). The Atmospheric module and the Land/Vegetation module

are based on the CESM-UCAR models CAM 5.3 and CLM 4.5 respectively and run at 1° lat-lon horizontal resolution, 46 vertical levels, while the Ocean and Sea-Ice models are respectively NEMO 3.4 and CICE 4.0 at ¼° lat-lon horizontal resolution, 50 vertical levels. The river routing model is based on the CESM-UCAR RTM model.

During the past year, the production of a large set of re-forecasts (hindcasts) required for model calibration and evaluation has also been completed for the Copernicus Climate Data Store. The whole set of ensemble hindcasts, in this case with 40 members for every start date, covers the period 1993-2016.

Based on such large dataset of re-forecasts, an overall evaluation of the SPS3 forecasting system has been produced, using methodologies most commonly used to assess the skill and the reliability of state-of-the-art seasonal prediction systems, both in terms of deterministic metrics (e.g., bias, anomaly correlation, etc) and probabilistic metrics (e.g., reliability diagrams, ROC score, ensemble statistics, dispersion, etc.). This evaluation of the SPS3 can be found in Sanna et al., 2017.

Figure 2.2 (based on the set of hindcasts provided to Copernicus as part of this project) shows the CMCC SPS3 skill in predicting NINO 3.4 index for forecast lead month 1 for the four main seasonal start dates, demonstrating the state-of-the-art capabilities of the CMCC SPS3 POP System.

In conclusion, CMCC is currently operating and developing a Global Seasonal Prediction System (CMCC SPS3) capable of producing global seasonal (six-month)

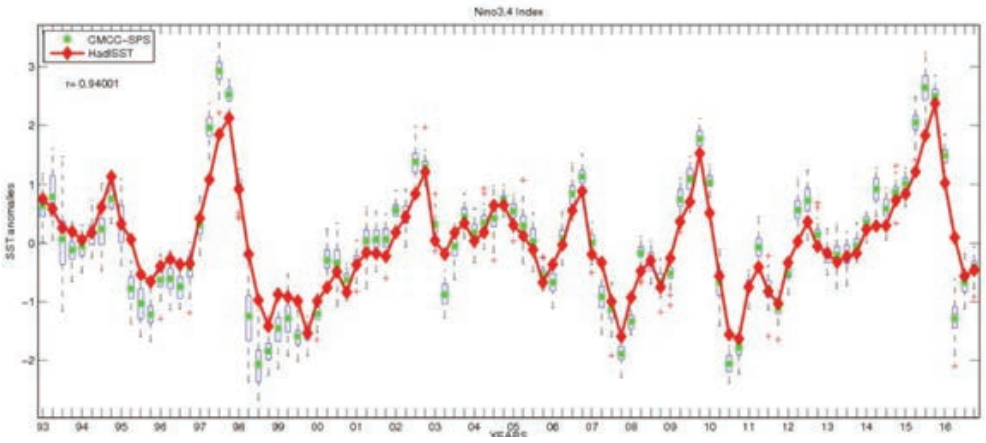

Fig, 2.2. NINO3.4 index predicted for lead 1 (one month ahead) on February, May, August and November start dates, years 1993–2016. The green dot identifies the forecast ensemble mean, the central mark indicates the median, and the bottom and top edges of the box indicate the 25th and 75th percentiles, respectively. The whiskers extend to the most extreme data points not considered outliers, and the outliers are plotted individually using the red '+' symbol. The red diamonds linked by the red line are the observed NINO3.4 anomalies as in the HadISST2 observations.

forecasts every first of the month and delivering them to Copernicus Data Store via the internet within a few days of the production start (6th of the month). A set of 24 years of hindcasts is also available in the Copernicus database to assess the performance of the system and to allow bias correction of operational forecasts.

References

Fogli, Pier Giuseppe, and D. Iovino, 2014: "CMCC–CESM–NEMO: Toward the New CMCC Earth System Model", CMCC Research Paper 248, available from https://www.cmcc.it/it/

Sanna et al., 2017: "CMCC-SPS3: The CMCC Seasonal Prediction System 3", CMCC Research Paper 285, available from https://www.cmcc.it/it/

Global multi-scale atmosphere model SL-AV

Mikhail Tolstykh[1,2], Rostislav Fadeev[1,2], Vladimir Shashkin[1,2] and Gordey Goyman[1,2]

[1] Marchuk Institute of Numerical Mathematics, Russian Academy of Sciences, Moscow, Russia
[2] Hydrometeorological Research Centre of Russia, Moscow, Russia
email: mtolstykh@mail.ru

Introduction

The appearance of first computers in the middle of XX century made the numerical weather prediction (NWP) possible. However, the numerical methods for solving the atmosphere equations had to be developed. Prof. Fedor Mesinger contributed greatly to the development of these methods; his textbook written in 1976 with Prof. A.Arakawa was translated into many languages and is now a compulsory element in teaching students. The limited area dynamical core based on primitive equations was developed in Belgrade in 1973, later it was transformed to the full operational NWP limited area model called Eta model.

Since then, the atmosphere models and their dynamical cores evolved, in particular, to use modern parallel computer architectures. Indeed, the common ways to improve the quality of numerical weather prediction and fidelity of the atmosphere model 'climate' are the increase of the atmospheric model resolution and advancements in parameterized description of unresolved subgrid-scale processes. Both ways imply the increase in computational complexity of the atmospheric models. Operational numerical weather prediction requires the forecast to be computed in few minutes per forecast day, while the climate modelling requires many multi-year runs to be completed in reasonable time. This means that the dynamical cores of the atmospheric models have to use efficiently thousands and tens of thousands processor cores.

We present here the SL-AV model used for numerical weather prediction and climate change modelling.

SL-AV model: current state

SL-AV is the global atmosphere model applied for the operational medium-range weather forecast at Hydrometeorological Research Center of Russia and as a component of the long-range probabilistic forecast system (Tolstykh et al 2015). It is also an atmospheric component of the coupled atmosphere-ocean-sea-ice model (Fadeev et al, 2016) use for climate change modelling. SL-AV is the model acronym (semi-Lagrangian, based on Absolute-Vorticity equation). The model is developed at Marchuk Institute of Numerical Mathematics, Russian Academy of Sciences (INM RAS) in

cooperation with the Hydrometeorological Research Centre of Russia (HMCR). The dynamical core of this model uses the semi-implicit semi-Lagrangian time-integration algorithm (Tolstykh et al, 2017). The specific features are the use of vorticity-divergence formulation and the application of fourth-order finite differences for approximation of non-advective terms of the equations. The dynamical core can use either regular or reduced latitude-longitude grids. Another feature of SL-AV is the possibility to use variable resolution in latitude. This approach is especially suitable for Russia territory which is stretched for almost 180° in longitude. Variable resolution in latitude with the ability to use non- equatorially symmetric grid reduction allows us to refine resolution in the region of interest (midlatitudes of Northern hemisphere) and to coarsen it in other regions (e.g. Southern hemisphere).

The parallel implementation of SL-AV model uses the combination of one-dimensional MPI decomposition and OpenMP loop parallelization (Tolstykh et al, 2017a). The model code is also adapted to run at Intel Xeon Phi processors (Tolstykh et al, 2017b).

Currently, the SL-AV code has 63 % parallel efficiency while using 9072 processor cores. The code is also able to use 13608 cores with the efficiency slightly higher than 50 %, for grid dimensions of 3024×1513×126 (the horizontal resolution of approximately 13 km). It is also important that the low-resolution version of the model (0.9×0.72 degrees in longitude and latitude respectively, 85 vertical levels) used for interannual predictability experiments computes the atmosphere circulation for 3 model years in less than 15 hours while using 180 processor cores.

Further development

Though there is room for further increase in scalability of SL-AV dynamical core, it has limitations, the hydrostatic approximation being the most severe one. This means that the horizontal resolution of the current dynamical core cannot be higher than 8-10 km. So the work has started on a new generation of this dynamical core. Some possible solutions will be discussed at the conference

References

Fadeev R.Yu., Ushakov K.V., Kalmykov V.V., Tolstykh M.A., Ibrayev R.A. (2016) Coupled atmosphere–ocean model SLAV–INMIO: implementation and first results. Russian J. Num. An. and Math. Mod. 31, 329-337, doi: 10.1515/rnam-2016-0031

Tolstykh M.A., Geleyn J.-F., Volodin E.M., Kostrykin S.V., Fadeev R.Y., Shashkin V.V., Bogoslovskii N.N., Vilfand R.M., Kiktev D.B., Krasjuk T.V., Mizyak V.G., Shlyaeva A.V., Ezau I.N., Yurova A.Y. (2015) Development of the multiscale version of the SL-AV global atmosphere model. Russ. Meteor. and Hydrol. 40, 374-382. doi: 10.3103/S1068373915060035

Tolstykh M., Shashkin V., Fadeev R., Goyman G. (2017a) Vorticity-divergence semi-Lagrangian global atmospheric model SL-AV20: dynamical core. Geosci. Model Dev. 10, 1961-1983 (2017), doi:10.5194/gmd-10-1961-2017.

Tolstykh M., Fadeev R., Goyman G., Shashkin V. (2017b) Further Development of the Parallel Program Complex of SL-AV Atmosphere Model. In: Voevodin V., Sobolev S. (eds) Supercomputing. RuSCDays 2017. Communications in Computer and Information Science, vol. 793, pp. 290-298. Springer, Cham (2017). doi: 10.1007/978-3-319-71255-0_23

Dynamical cores for the Met Office's Unified Modelling system: Past, present and future

Nigel Wood
Met Office, Exeter, EX1 3PB UK
(nigel.wood @metoffice.gov.uk)

The past: New Dynamics

In 2002 the dynamical core colloquially referred to as the New Dynamics (Davies et al. 2005) was implemented into operations at the Met Office. This represented a major step towards the unification of all the Met Office's modelling systems since it allowed the regional, or limited-area, models to use the same dynamical core as both the operational global NWP model and the global climate prediction model.

Since then there has been a coordinated drive towards `seamless modelling' in which there has been progressive unification of the physical parametrization schemes used in all these models. Such an approach has a number of advantages but comes also with a number of challenges. These are detailed and discussed by Brown et al. (2012).

There are various challenges for a dynamical core if it is to work effectively and efficiently across all spatial scales from O(1 km) to O(10,000 km) and across all temporal scales from a few minutes to centuries, whilst also being able to deliver operational global forecasts within one hour of model initiation. For it to be accurate at the mesoscales required for regional modelling, the model was chosen to be nonhydrostatic; to be accurate at the largest planetary scales the model had to be compressible (Davies et al. 2003). Together these choices meant that the model admits the fast acoustic modes. To avoid the time step being restricted by the frequency of the acoustic modes, a two-time level, semi-implicit temporal discretization was implemented.

A global model also needs to be able to maintain, and accurately represent the adjustment to, large scale hydrostatic and geostrophic balances. This suggests the use of certain grid staggerings for the finite-difference spatial discretization, specifically the Arakawa C-grid in the horizontal coupled with the Charney-Phillips grid in the vertical. Good balance was also helped by the choice to use a two-time step semi-implicit scheme (Cullen 2007).

A further design criterion for the New Dynamics was to reduce, as far as was then considered possible, the numerical diffusion required to keep the model stable and noise free. The two-time level, semi-implicit scheme for temporal aspects and the choice of staggering for spatial aspects both helped in this regard as they eliminated many of the compu-

tational modes associated with alternative choices. But the presence of the polar singularity in the latitude-longitude grid remained a source of noise. A key element in mitigating this source, as well as enhancing the efficiency of the model through allowing a long time step, was the use of a semi-Lagrangian transport scheme for nearly all variables.

The only variable that did not use the semi-Lagrangian scheme was the dry density for which a semi-implicit form of an Eulerian flux scheme was used. This was to ensure that the dry mass of the atmosphere was conserved exactly throughout even the longest climate simulations.

The present: ENDGame

The New Dynamics successfully met a number of challenges presented by the aim of unification of the models across all scales. However, like many dynamical cores its development took a number of years and over that time research and experience at other NWP centres had continued apace. Additionally, as the resolution of the models continued to increase, numerical instabilities due to the dynamical core became more of an issue. This led to a number of short term, tactical mitigations to maintain operational robustness. This compromised some of the original design aims, particularly that to keep numerical diffusion to a minimum. To address these issues a program of research and development started in 2002 and continued until 2014 when the Even Newer Dynamics for General atmospheric modelling of the environment (ENDGame) replaced the New Dynamics as the dynamical core of the Met Office's Unified Model.

As its acronym suggests, ENDGame (Wood et al. 2014) was an evolution of the New Dynamics. It aimed to maintain the beneficial features of the previous model, specifically: the almost unapproximated continuous equation set (the deep-atmosphere, nonhydrostatic Euler equations); the two time-level semi-Lagrangian semi-implicit (SISL) discretization; and the Arakawa-C horizontal, and Charney-Phillips vertical, grid staggering. However, the method of solution of the target SISL discretization was radically changed with the introduction of a nested iterative scheme, similar to that implemented in the Canadian GEM model by Côté et al. (1998). In this approach the semi-Lagrangian transport scheme is handled in an outer loop in which, as the outer-loop iterations increase, the winds used to compute the Lagrangian trajectory approach a centred average of the winds from the beginning and the end of the trajectory (and hence approach second-order accuracy). At the heart of the inner loop is a relatively simple, linear Helmholtz problem, the solution to which provides the semi-implicit update to the pressure field. To achieve a simple (7-point stencil) Helmholtz problem, the non-linear terms, the Coriolis terms and the orographic terms are evaluated as source terms for the linear Helmholtz equation. These source terms are averaged along the model trajectory using the latest known estimates for the next time-level model state. As the inner-loop iterations increase, the handling of these terms approaches the target SISL scheme.

Additionally, the Eulerian flux form handling of the dry density equation was replaced with a semi-Lagrangian

approach. This means that the whole model state is transported in a more coherent semi-Lagrangian manner and, consequently, it removes a source of numerical instability. However, it means that the model no longer conserves dry mass in a local sense and a global mass fixer has to be applied.

Another important change for the global implementation of ENDGame was to shift the placement of the model variables in the meridional direction so that the only variable stored at the two singular polar points is the meridional wind component. This improves the handling of wave propagation across the poles (Thuburn and Staniforth 2004) and also simplifies considerably the solution of the Helmholtz problem on the globe.

The combination of these changes meant that the off-centring applied in the semi-implicit implementation was considerably reduced (from values ranging from 0.7 to 1.0, to a value of 0.55, where 0.5 represents a centred, second-order scheme). This improved the variability of the model (by reducing the temporal damping). Further, despite the reduction in damping, the stability of the model improved significantly (Walters et al. 2017).

A somewhat unexpected consequence of these changes (mainly those to the Helmholtz problem and the staggering of variables near the poles), that was not specifically the target of the redesign, was that the new model has much improved scalability. This turned out to be a critical aspect of ENDGame since its improved scalability was necessary to be able to increase the global model (meridional) resolution from 25km to 17km. The current global resolution is 10km.

The future: GungHo

As already noted, the design of ENDGame (initiated in 2002) was focused on improving the Unified Model's accuracy and stability and not specifically its scalability. So in 2010, as the trend towards ever more massively parallel computers began to bite, it was recognized that in order to remain competitive into the future the model's dynamical core had to become much more scalable. As a result a 5 year project was initiated that was joint between the Met Office, UK academics (funded by NERC, the UK Natural Environment Research Council) and scientists from the UK's Science and Technology Facilities Council (STFC). The project became known as GungHo.

From the beginning it was recognized that the principal driver for a further redesign of the dynamical core was the future of computer architectures. Therefore, co-design of the model with computational science experts was an essential element of the project, and remains so today.

It was clear even before the start of the project that the principal bottleneck to achieving good scalability was the polar singularities of the latitude-longitude mesh employed in the Unified Model. In the current 10km global model, the latitudinal spacing between the row of grid points nearest each pole is a mere 13 m. This spacing reduces quadratically with increased resolution and so would be only 13 cm (centimetres!) for a 1km global model.

This presents two impediments to scaling. The first is that the condition number for the Helmholtz problem scales as the ratio of the largest to the smallest

length scales and hence this increases linearly with increasing resolution. This means that the number of iterations of the Krylov solver increases with resolution and hence also the amount of both local and global communication. The second is that for a given wind speed the latitudinal, or zonal, Courant number in the region of the poles also increases linearly with resolution. This leads to the requirement of more and more remote communication (in computational space).

Therefore, a principal aim of GungHo was to decide on an alternative mesh to the latitude-longitude one used by ENDGame. One of the early outputs from the GungHo project was the review by Staniforth and Thuburn (2012) of various alternative meshes available, together with their pros and cons. There was no shortage of options! However, the real challenge of GungHo was to move away from the latitude-longitude mesh whilst retaining the beneficial accuracy and stability of the ENDGame dynamical core. One aspect of this was avoiding reintroducing computational modes (that would require numerical diffusion to control). This led to the preferred adoption of a quadrilateral mesh. (It is termed here a `preferred' option since an element of GungHo's risk management is to maintain different options for as long as possible rather than definitively deciding on one early on.)

At the beginning of GungHo a survey of the model users was undertaken to ask what their main requirements of the dynamical core were. Of the few replies received, by far the dominant requirement was improved, more local, mass conservation. This consideration together with the choice of a quadrilateral mesh led to the adoption of the cubed-sphere mesh rather than the alternative quadrilateral mesh known as Yin-Yang. In particular a non-conformal cubed-sphere was chosen in order to avoid the reintroduction of pole-like singularities at the corners.

A consequence of being non-conformal is that the coordinate lines are not orthogonal to each other. In contrast to the latitude-longitude mesh this presents a number of challenges to achieving many of the `essential and desirable properties of a dynamical core' listed and discussed in Staniforth and Thuburn (2012). In this regard, an advantage of finite-element schemes is that their numerical properties are less dependent on the orthogonality of the mesh than finite-difference ones of the same order. That said though, many finite-element approaches share the disadvantages of co-located grids (e.g. the Arakawa-A grid) in terms of their numerical wave dispersion properties and also computational models (e.g. Melvin et al. 2012). Therefore, the choice was made for GungHo to adopt the mixed finite-element method (e.g. Cotter and Shipton 2012). In this approach a number (one more than the spatial dimension) of different function spaces are used and by making judicious choice of those spaces and which variables to store in which space, the beneficial properties of the C-grid staggering can be obtained (specifically, the necessary conditions for no computational modes and the ability to maintain geostrophic balance). The choice of spaces and variables assigned to those spaces comes from consideration of exterior calculus and aspects of differential geometry (e.g. Cotter and

Thuburn 2014) and is chosen so that the appropriate differential operator maps from one space onto the kernel of the next space.

This approach was found to work well for the shallow-water equations. Extension to three dimensions was relatively straightforward with the exception that, whilst in three dimensions the Lorenz vertical staggering of the buoyancy variable fits very naturally into the method, the Charney-Phillips staggering does not. However, a method using an appropriate scalar space was found and shown to provide the same benefit as for a finite-difference model (Melvin et al. 2018a).

An important element of any dynamical core is its transport scheme. From the user survey local conservation is an important consideration and suggested some form of flux scheme. Additionally, a significant contributor to the improvement in performance of dynamical cores over the last few decades has been the adoption of upstream biased schemes. These have good dispersion properties together with the benefit of limited, but scale-selective, damping. In contrast, it is beneficial for those parts of the dynamical core that are responsible for wave propagation to be handled in a centred manner and with relatively low order, typically second order (Holdaway et al. 2008). It was therefore considered essential for GungHo to retain the flexibility to use some form of finite-volume flux-form transport scheme independently of the choice of the particular mixed finite-element method chosen. This requires a conservative mapping between the finite elements and the appropriate finite volumes. Using (the target) lowest-order finite elements this mapping is trivial and the approach has been shown to be effective for an Eulerian scheme (the implementation of a semi-Lagrangian flux form is underway). It remains to be seen whether the proposed technique can be extended successfully to allow coupling to higher-order mixed finite elements.

In summary, the proposed GungHo design is a semi-implicit temporal discretization of a mixed finite-element spatial discretization coupled with a flux-form finite-volume transport scheme. Early results are promising (e.g. Melvin et al. 2018b) and testing is now being extended to include the Unified Model's physical parametrizations (coupled to GungHo in the same way as the transport scheme is).

Future proofing: LFRic

An important aspect of future-proofing the design of GungHo was the deliberate choice to keep as many options open as possible. Specifically, a decision was made to use indirect addressing in the horizontal (exploiting the columnar nature of the mesh to amortize the cost of the indirect addressing). This approach makes it a lot easier (in principle at least!) to radically change the choice of mesh without having to redesign and rewrite the whole model. Additionally, although the target is a low-order finite-element scheme, the option to use higher orders has been retained. This is because it might be a way of reducing any undue grid imprinting due to the corners and edges of the sphere and it would also be necessary (to retain the desired numeri-

cal properties) if a triangular mesh were ever implemented.

The original motivation for GungHo was to improve the scalability of the Unified Model's dynamical core. However, as time has progressed it has become evident that not only are supercomputers providing more and more cores (and hence the scaling problem) but the nature of those cores is also changing (principally to address the energy problem). The architectures are becoming more and more heterogeneous (for example as GPUs become incorporated into CPUs). And those processors are supported by deeper and deeper hierarchies of memory. Further, no one seems able or willing to predict exactly what the architectures of the mid-2020s and beyond will look like. It is becoming essential therefore that, whatever the scientific design of the dynamical core, its technical implementation must be, as far as possible, agnostic about the architecture that it is designed for.

This realization came at a time when it became clear that to implement GungHo within the Unified Model would require two major changes. The first would be a move away from the simple tensor-product indexing afforded by the use of a latitude-longitude mesh to indirect addressing. The second would be the move away from the finite-difference scheme to a finite-element scheme. The Unified Model had been fundamentally built and designed around direct addressing and finite-difference numerics. Additionally, it was originally designed some 25 years ago. The bold decision was therefore made to design, develop and implement a new model infrastructure with the specific aim of being as agnostic as possible about the supercomputer architectures. This project is a joint project between the Met Office and STFC and it is called LFRic after Lewis Fry Richardson who made the first steps towards numerical weather prediction decades before the first computers were available.

At the heart of LFRic is an implementation (named PSyKAl) of the principle of a `separation of concerns'. In this approach, a model time step is separated into three layers: Parallel Systems; Kernels; and Algorithms. In the Algorithm layer only global fields are manipulated without any reference to specific elements of those fields. The Kernel layer operates on whatever the smallest chunk of model memory is. For LFRic this is currently a single column of data. It is the job of the PSy layer to dereference the specific elements of the global fields and ensure that they are distributed appropriately to the relevant pieces of computational hardware. Therefore, it is the PSy layer that implements all the calls to MPI, including the necessary halo exchanges etc., and that also implements the directives for OpenMP, including colouring where necessary (to avoid contentions). Work is underway to extend PSy further to allow implementation of OpenACC.

This approach means that a natural scientist does not need to worry about how to implement whatever specific aspects are required to make the model run on a parallel machine. This makes the parallel aspects less prone to programming error by scientists and it also avoids the habit of many scientists of putting in redundant halo exchanges 'just in case' with the associated inefficiencies.

The key aspect of this approach is that the PSy layer is autogenerated by a Python script called PSyclone, owned and developed by STFC. This relies on there being a strict API between each of the layers together with appropriate, supporting metadata. This aspect is key because it means that there is only one source code independently of the type of supercomputer that any particular simulation is run on. Additionally, any generic or machine-specific optimizations can be encoded within PSyclone, again without polluting the Algorithms and the Kernels where the natural scientists work. As well as being flexible in terms of future supercomputer architectures, the approach also means that the model can be run efficiently across a range of contemporaneous architectures without requiring invasive changes to the source code.

As an illustration of the effectiveness and utility of this approach, it took less than two weeks for the original, serial version of GungHo to be able to run in parallel on 220,000 cores Met Office Cray XC40 once it was coupled to PSyclone.

Summary

Developing a dynamical core that is suitable for operational, unified modelling across spatial scales ranging from below 1km urban scales to planetary scales, and across temporal scales ranging from a few minutes to centuries, is challenging. It puts strong constraints on both the continuous equation set used and the combination of numerical methods used to discretize those equations. In this regard, the semi-implicit semi-Lagrangian scheme applied to the almost unapproximated deep-atmosphere, nonhydrostatic equations has served the Met Office well for over 15 years.

An emerging additional challenge is to make the model scalable when run on the massively parallel supercomputers of today, as well as ensuring that the models will continue to be efficient on whatever the next generation of supercomputer architectures will look like.

The combination of the GungHo dynamical core with the LFRic modelling framework attempts to rise to those challenges. The result is a mixed finite-element, finite-volume, semi-implicit scheme implemented within a modern, flexible, object-oriented, software infrastructure designed using the concept of a separation of concerns.

Acknowledgments

The development and implementation of the three dynamical cores and associated modelling systems discussed here represent the efforts of a large number of people. It is a pleasure to acknowledge their dedication and efforts. In particular, the author would like to thank all members of the Met Office's Dynamics Research team, both past and present, as well as the members of both the GungHo and LFRic teams. Thanks also go to Tom Melvin for his helpful comments on a draft of this manuscript.

References

Adams Samantha, Rupert Ford, Matthew Hambley, James Michael Hobson, Iva Kavcic, Christopher Maynard, Thomas Melvin, Eike Mueller, Steve Mullerworth, Andrew Porter, Mike Rezny, Ben Shipway, Ricky

Wong (2018) LFRic: Meeting the challenges of scalability and performance portability in weather and climate models, submitted to the Journal of Parallel and Distributed Computing: Exascale Applications and Software

Brown A., S. Milton, M. Cullen, B. Golding, J. Mitchell, A. Shelly (2012) Unified modeling and prediction of weather and climate: a 25-year journey, Bull. Amer. Meteor. Soc., 93, 1865-1877

Côté J., S. Gravel, A. Méthot, A. Patoine, M. Roch, A. Staniforth (1998) The operational CMC-MRB Global Environmental Multiscale (GEM) model. Part I: Design considerations and formulation, Mon. Wea. Rev., 126, 1373-1395

Cotter C. J. and J. Shipton (2012) Mixed finite elements for numerical weather prediction, J. Comput. Phys., 231, 7076-7091

Cotter C. J. and J. Thuburn (2014) A finite element exterior calculus framework for the rotating shallow-water equations, J. Comp. Phys., 257, 1506-1526

Cullen M. J. P. (2007) Modelling atmospheric flows, Acta Numerica, 16, 67-154

Davies T., A. Staniforth, N. Wood and J. Thuburn (2003) Validity of anelastic and other equation sets as inferred from normal-mode analysis, Q. J. R. Meteorol. Soc., 129, 2761-2775

Davies T., M. Cullen, A. Malcolm, M. Mawson, A. Staniforth, A.A. White and N. Wood (2005) A new dynamical core for the Met Office's global and regional modelling of the atmosphere, Q. J. R. Meteorol. Soc., 131, 1759-1782

Holdaway Dan, John Thuburn and Nigel Wood (2008) On the relation between order of accuracy, convergence rate and spectral slope for linear numerical methods applied to multiscale problems, Int. J. Num. Meth. Fluids, 56, 1297-1303

Melvin T., A. Staniforth and J. Thuburn (2012) Dispersion analysis of the Spectral Element Method, Q. J. R. Meteorol. Soc., 138, 1934-1947

Melvin T., T. Benacchio, J. Thuburn, C. Cotter (2018a) Choice of function spaces for thermodynamic variables in mixed finite element methods, Q. J. R. Meteorol. Soc., To appear

Melvin T., T. Benacchio, B. Shipway, N. Wood, J. Thuburn and C. Cotter (2018b) A mixed finite-element, finite-volume, semi-implicit discretisation for atmospheric dynamics: Cartesian geometry, Q. J. R. Meteorol. Soc., In preparation

Staniforth A. and J. Thuburn (2012) Horizontal grids for global weather prediction and climate models: a review, Q. J. R. Meteorol. Soc., 138, 1-26

Thuburn J. and A. Staniforth (2004) Conservation and linear Rossby-mode dispersion on the spherical C Grid, Mon. Wea. Rev., 132, 641-653

Walters D., I. Boutle, M. Brooks, T. Melvin, R. Stratton, S. Vosper, H. Wells, K. Williams, N. Wood, T. Allen, A. Bushell, D. Copsey, P. Earnshaw, J. Edwards, M. Gross, S. Hardiman, C. Harris, J. Heming, N. Klingaman, R. Levine, J. Manners, G. Martin, S. Milton, M. Mittermaier, C. Morcrette, T. Riddick, M. Roberts, C. Sanchez, P. Selwood, A. Stirling, C. Smith, D. Suri, W. Tennant, P. L.

Vidale, J. Wilkinson, M. Willett, S. Woolnough and P. Xavier (2017) The Met Office Unified Model Global Atmosphere 6.0/6.1 and JULES Global Land 6.0/6.1 configurations, Geosci. Model Dev., 10, 1487-1520

Wood N., A. Staniforth, A. White, T. Allen, M. Diamantakis, M. Gross, T. Melvin, C. Smith, S. Vosper, M. Zerroukat and J. Thuburn (2014) An inherently mass-conserving semi-implicit semi-Lagrangian discretization of the deep-atmosphere global non-hydrostatic equations, Q.J.R. Meteorol. Soc., 140, 1505-1520

Towards revision of conventional theory and modelling of turbulence in boundary-layer flows

Sergej S. Zilitinkevich[1,2,3] *and Evgeny Kadantsev*[1,2]

[1] Finnish Meteorological Institute
[2] University of Helsinki
[3] University of Nizhny Novgorod

Abstract

Vital feature of weather and climate close to Earth's surface is high level of turbulence. A mosaic of essentially turbulent boundary layer flows covers the globe and provides comfortable habitat for terrestrial biosphere and the humankind. Especially turbulent are weather and climate over complex topography, vegetation and, especially, over urban canopies due to the very high roughness – enhancing the shear-generated turbulence, and anthropogenic warming – enhancing the buoyancy-generated turbulence.

Until now, comprehending and modelling of turbulence employ old turbulence-closures conceptually originated from Kolmogorov (1942) and based on the sole use of turbulent kinetic energy (TKE) budget equation, neglecting turbulent potential energy (TPE) and conversions of TKE into TPE and vice versa.

Common reluctance to revise traditional turbulence closures is not surprising. Their major drawbacks root in the vision of turbulence based on the paradigm attributed to Kolmogorov (1941-1942). Hence, revision of turbulence closures factually implies the revision of paradigm universally recognised over decades. We emphasise that Kolmogorov considered only shear-generated turbulence in neutrally stratified flows, where his major postulates: (i) strictly forward energy cascade (from larger to smaller eddies – towards dissipation), and (ii) strictly down-gradient turbulent fluxes (along the mean gradient of transporting property) are justified. Moreover, Kolmogorov was not responsible for extension of his vision of turbulence to stratified flows. This has been made by his followers without proof.

This talk highlights inconsistencies of conventional paradigm as applied to essentially stratified turbulence; demonstrates miscarriages of traditional approach; outlines novel Energy- and Flux-Budget (EFB) turbulence-closure theory accounting for non-gradient turbulent transport and demonstrates capability of the proposed closure to realistically reproducing stably stratified atmospheric boundary layers poorly modelled by any other turbulence closures.

References

Kolmogorov A., 1941a: The local structure of turbulence in incompressible viscous fluid for very large Reynolds number (in Russian), *Dokl. Akad. Nauk SSSR*, **30**, 301. (English translation, Friedlander S. and Topper L., *Turbulence*, Interscience, New York, 1961.)

Kolmogorov A., 1941b: Dissipation of energy in locally isotropic turbulence, *Dokl. Akad. Nauk SSSR*, **31**, 538.

Kolmogorov A., 1942: Equations of turbulent motion of an incompressible turbulent fluid, *Izv. Akad. Nauk SSSR* Ser. Phys. **VI**, No. l-2, p. 56.

Monin A., Obukhov A., 1954: Basic laws of turbulence mixing in the surface layer of the atmosphere. Trudy Geofiz. Inst. AN SSSR, 24 (151), 163-187.

Zilitinkevich, S.S., 1973: Shear convection. *Boundary-Layer Meteorol.*, **3**, 416-423.

Zilitinkevich S.S., Hunt J.C.R., Grachev A.A., Esau I.N., Lalas D.P., Akylas E., Tombrou M., Fairall C.W., Fernando H.J.S., Baklanov A., Joffre S.M., 2006: The influence of large convective eddies on the surface layer turbulence. *Quart. J. Roy. Met. Soc.* **132**, 1423-1456.

Zilitinkevich S.S., 2013: *Atmospheric Turbulence and Planetary Boundary Layers*. Fizmatlit, M., 248 pp.

Zilitinkevich S., Elperin T., Kleeorin N., Rogachevskii I., Esau I., 2013: A hierarchy of energy- and flux-budget (EFB) turbulence closure models for stably stratified geophysical flows. *Boundary-Layer Meteorol.* **146**, 341-373.

Contents

Српска академија наука и уметности захваљује се на финансијској подршци:
Serbian Academy of Sciences and Arts thanks the following for their financial support:

МИНИСТАРСТВО ПРОСВЕТЕ,
НАУКЕ И ТЕХНОЛОШКОГ РАЗВОЈА

Републички
хидрометеоролошки
завод Србије

Институт за
водопривреду
”Јарослав Черни”